

NATIONAL ADVISORY COMMITTEE FOR AERONAUTICS

WARTIME REPORT

ORIGINALLY ISSUED

March 1943 as
Advance Restricted Report

AN INVESTIGATION OF AIRCRAFT HEATERS

IX - MEASURED AND PREDICTED PERFORMANCE OF TWO EXHAUST
GAS-AIR HEAT EXCHANGERS AND AN APPARATUS FOR
EVALUATING EXHAUST GAS-AIR HEAT EXCHANGERS

By L. M. K. Boelter, M. A. Miller, W. H. Sharp,
E. H. Morrin, H. W. Iversen, and W. E. Mason
University of California



WASHINGTON

NACA WARTIME REPORTS are reprints of papers originally issued to provide rapid distribution of advance research results to an authorized group requiring them for the war effort. They were previously held under a security status but are now unclassified. Some of these reports were not technically edited. All have been reproduced without change in order to expedite general distribution.

NATIONAL ADVISORY COMMITTEE FOR AERONAUTICS

ADVANCE RESTRICTED REPORT

AN INVESTIGATION OF AIRCRAFT HEATERS

IX - MEASURED AND PREDICTED PERFORMANCE OF TWO EXHAUST
GAS-AIR HEAT EXCHANGERS AND AN APPARATUS FOR
EVALUATING EXHAUST GAS-AIR HEAT EXCHANGERS

By L. M. K. Boelter, M. A. Miller, W. H. Sharp,
E. H. Morrin, H. W. Iversen, and W. E. Mason

SUMMARY

Laboratory tests have been conducted to determine the thermal output and the pressure drop characteristics of the Airesearch and Solar fluted-type exhaust gas-air heat exchangers. The apparatus employed in these tests consists of a natural gas furnace of 3,000,000 Btu per hour thermal capacity, a centrifugal blower for delivering combustion air to the furnace and ventilating air to the heat exchanger under test, together with a system of ducting and various measuring devices. With this test stand, exhaust gas and ventilating air can be circulated through the heat exchanger under test at flow rates of 8500 and 6500 pounds per hour, respectively, at an exhaust gas temperature of 1600° F.

It was found that at exhaust gas and ventilating air flow rates of 7000 and 5000 pounds per hour, respectively, the thermal output of the Airesearch heat exchanger was about 320,000 Btu per hour while that of the Solar unit was about 170,000 Btu per hour. This difference in output is accounted for largely in the much greater area of heat transfer surfaces in the Airesearch heat exchanger. In the analysis of the test data the measured thermal outputs and pressure drops of the two heat exchangers are compared with predicted values.

INTRODUCTION

From the results of previous experimental tests (reference 1) on double tube heat exchangers, using both an internal combustion engine and a natural gas burner for the generation of hot exhaust gas, it was apparent that the thermal and pressure-drop data were nearly independent of these two means of exhaust gas generation. The latter method was therefore used in the test stand described in this report since it offered fewer operational difficulties. The previous tests were made on a somewhat smaller test stand than that employed in the present test program.

The tests described in this report, a part of an extensive investigation on the development of aircraft heaters now being conducted in the Mechanical Engineering Laboratory of the University of California, was sponsored by and conducted with financial assistance from the National Advisory Committee for Aeronautics. Results of this investigation already completed are contained in eight NACA advance restricted reports, which have the general title: "An Investigation of Aircraft Heaters."

HEAT EXCHANGER TEST APPARATUS

The laboratory heat exchanger testing apparatus employed in the tests described in this report consists of a natural gas furnace and a centrifugal blower which supplied both the combustion air to the furnace and the ventilating air to the heat exchanger being tested, together with ducting and measuring devices. A schematic sketch of this heater test stand is shown in figure 1. Photographs of various essential parts of the apparatus are shown in figures 2 to 5.

The blower, which is a radial-vane, open-runner, single-stage Kennedy type, is driven by a 30-horsepower electric motor operating at about 3600 rpm. The delivery pressure of the blower is quite constant throughout the operating range at approximately $1\frac{2}{3}$ pounds per square inch. The blower is capable of delivering a flow of about 6500 pounds per hour of ventilating air and about 8500 pounds per hour of air to the gas furnace for the generation of exhaust gas.

The gas furnace has a thermal output of about 3,000,000 Btu per hour. With the exhaust gas and ventilating air flow rates indicated, the temperature of the exhaust gas is about 1600° F.

The air from the blower is discharged into a 12-inch manifold and thence into two 8-inch ducts which supply combustion air to the furnace and the ventilating air to the heat exchanger, as shown in figure 1.

Part of the combustion air is conducted to the bottom of the furnace where it reacts with the natural gas in a special burner head. The remainder of the air, called the "cooling air," is bypassed to the top of the combustion chamber where it mixes with the hot gases from the burner and acts as a "temperature regulator," cooling the gases to the desired operating temperature. The furnace is part of a standard Besler automatic flash-type steam boiler. The boiler tube section was replaced by a conical top containing a specially designed chamber for the mixing of the hot combustion gases and the "cooling air." (See figs. 3 and 5.)

The mixing chamber, of the gas furnace, shown in figure 6, consists of a converging section which conducts the "cooling air" to a point near the exit of the furnace where, by a sudden expansion, the "cooling air" is mixed with the hot gases from the combustion chamber below. When the test stand was first operated, difficulty was experienced in obtaining a uniform temperature distribution in the exhaust gases leaving the furnace. After many experiments the mixing device described above was adopted, since it was a compromise between better mixing with a large pressure drop and poorer mixing which produced a smaller loss in pressure. An example of the latter case was given by a set of five spiral vanes equally spaced around the periphery of the 8-inch duct immediately downstream from the furnace. Very little mixing occurred for the vanes merely twisted the temperature distribution around the axis of the pipe. Good mixing, but large pressure drops, was accomplished by the mixing device shown in figure 7 which was placed in the 8-inch duct downstream from the furnace.

An annulus of $1\frac{1}{2}$ inches existed between the outside of the perforated cylinder and the inside of the 8-inch duct. The mixture of hot gases and cool air passed into the interior of the cylinder and then was caused to rotate, by a spiral vane,

through 360° and to pass continuously into the annulus through the many perforations. The mixture then passed into the 8-inch pipe by a sudden expansion from the $1\frac{1}{2}$ -inch annulus. Thus a given mass of gas and air was distributed around the perimeter of the duct and was further mixed by the sudden expansion into the 8-inch duct. The disadvantageous pressure drops were decreased by placing holes in the end of the cylinder, but this eliminated the sudden expansion and thereby decreased the effectiveness of the mixer. In most cases the exhaust gas temperature (deg F) is uniform across the gas stream within five percent when the mixing device shown in figure 7 is used.

The combustion chamber of the gas furnace operates at a pressure of about one pound per square inch. The ignition of the combustible gases is caused by a spark from a 10,000 volt transformer. A safety valve, which consists of an 8-inch diameter vertical standpipe capped by a weight-loaded disk, was installed immediately upstream from the furnace. (See fig. 5.) The valve opens at a pressure of two pounds per square inch. It has proved successful on a few occasions when the flame in the furnace was inadvertently extinguished and suddenly reignited.

The heater test section is located 7 feet downstream from the furnace and mixing chamber. The inlet and outlet exhaust gas ducts are 8 inches in diameter, while the ventilating air ducts are 5 inches in diameter. The heater being tested is mounted between flanges whenever possible, but occasionally special slip joints are necessary. A sliding joint is used on the exhaust gas side downstream from the heater in order to allow for thermal expansion of the heater and ducting.

The rate of flow of ventilating air to the heat exchanger is metered by means of a 5-inch orifice. The combustion air flow is metered by a 6-inch orifice. These orifices are installed in the two 8-inch air ducts as shown in figure 1.

The total weight rate of exhaust gas is determined by adding the weight rate of natural gas to the weight rate of combustion air. The orifices were fabricated in accordance with the A.S.M.E. metering specifications (reference 2) and were calibrated by means of a Prandtl type pitot-static tube. Smaller orifices are available to obtain greater accuracy at low weight rates. Straight sections of 8-inch duct are placed for more than 20 pipe diameters upstream

and more than 8 pipe diameters downstream from the orifices, corresponding to standard A.S.M.E. motoring procedure. Two sets of radius pressure taps are installed at each orifice. The taps are located one pipe diameter upstream and one-half pipe diameter downstream from the orifice. A small manifold was constructed so that either or both sets of static pressure taps could be connected across the metering manometers. (See fig. 4.)

The natural gas is metered by means of an 0.875-inch sharp-edge orifice in a 2-inch pipe at a pressure of 5 pounds per square inch. This pressure is reduced to about 1 pound per square inch at the combustion chamber.

The temperature of the exhaust gas entering and leaving the heater is measured by means of traversing shielded thermocouples (reference 3). The thermocouple junction must be shielded in order to eliminate the cooling effect, by radiation, when the junction "sees" the relatively cool duct walls (fig. 9). The outlet gas temperature is usually measured about 30 inches downstream from the heater in order to provide for vanes in the duct which mix the exhaust gases leaving the heater. Asbestos lagging on the air and gas ducts minimizes the heat transfer to or from the surroundings or ducts.

From the exhaust gas temperature traverses made at the heat exchanger inlet and outlet, the mixed mean temperatures at these points were computed. This practice has been found necessary because large discrepancies are introduced into the heat balance computations by small errors in computed mixed mean exhaust gas temperatures.

Temperatures of the ventilating air are measured by means of traversing thermocouples also. The location of these thermocouples is usually determined by the configuration of the air shroud. A $3\frac{1}{2}$ -inch diameter orifice in the 5-inch ventilating air outlet duct is used to mix the air stream in order to obtain a uniform temperature distribution (within 3 percent in deg F) at this point.

Temperature measurements of the two surfaces throughout the heater are also obtained. The thermocouples are usually welded to the heater metal and are insulated from the air stream by means of porcelain tubing to decrease the error due to conduction of heat along the wires.

All of the thermocouples are made of chromel and alumel wire (18 to 28 gauge). "Auxiliary" junctions are eliminated by using chromel-alumel lead wires throughout the circuits.

The thermocouple voltages were measured by utilizing a laboratory potentiometer with the thermocouple cold junction maintained at 32° F by immersion in an ice-filled thermos jug.

Static pressure drop across the air and exhaust gas sides of the heat exchangers was measured by means of four pressure taps before and after the test section. Each of these four pressure taps is equipped with a shut-off cock so that the pressure distribution around the periphery can be observed. For the tests on the Airesearch heat exchanger the pressure taps on the exhaust gas side were installed 10 inches before and after the heat exchanger. Those on the ventilating-air side were placed 8 inches before and after the inlet and outlet header openings. For the tests on the Solar heat exchanger the pressure taps on the exhaust-gas side were placed 16 inches before and 10 inches after the heated section. Those on the ventilating air side of the heater were placed 24 inches before and after the heated section. The presence of the ventilating air shroud caused these differences in the locations of the pressure taps.

The metering and pressure drop manometers are mounted on the panel shown in figure 4. The following measurements which are obtained by each manometer reading from left to right in figure 4 are:

1. Static pressure upstream from ventilating air orifice
2. Differential pressure across ventilating air orifice
3. Static pressure upstream from combustion air orifice
4. Differential pressure across combustion air orifice
5. Static pressure upstream from natural gas orifice
6. Differential pressure across natural gas orifice
7. Static pressure of natural gas after reducing valve
8. Pressure drop across ventilating air side of heater
9. Pressure drop across exhaust gas side of heater

Manometers are also located at the discharge and suction sides of the air blower.

The flow of ventilating air, combustion air to the lower part of the furnace, and cooling air to the top of the furnace are controlled by 8-inch butterfly valves. The $1\frac{1}{2}$ -inch butterfly valve

which controls the flow of natural gas is connected to the 8-inch butterfly valve which controls the flow of combustion air in order to maintain approximately constant air-to-fuel ratios in the combustible mixture. (See fig. 3.)

DESCRIPTIONS OF HEAT EXCHANGERS

The Airesearch heat exchanger is a parallel flow, unfinned, fluted-type unit containing 48 alternate exhaust-gas and ventilating air passages. The over-all length of the heat transfer surface is 26 inches. A diagram of the heater is shown in figure 9 and photographs of its arrangement in the test stand are shown in figures 10, 11, and 12.

The Solar heat exchanger is similar in general design to the Airesearch type except that it contains 32 alternate exhaust gas and ventilating air passages and has a heating section length of $19\frac{1}{2}$ inches. The Solar heat exchanger is shown in figures 13 to 16.

The shrouds by which the ventilating air entered and exited from the heat exchangers were obtained from the Ames Aeronautical Laboratory of the NACA at Moffett Field, Calif. The inlet ducts of each of these air shrouds contained turning vanes to distribute the flow of air uniformly around the periphery of the heat exchanger. The outlet headers were not equipped with turning vanes. The effectiveness of these vanes was observed by studying the results of velocity distribution measurements made by a Prandtl type pitot-static tube.

SYMBOLS

- A area of heat transfer, ft^2
- c_{pa} heat capacity of air at constant pressure, $\text{Btu/lb } ^\circ\text{F}$
- c_{pg} heat capacity of exhaust gas at constant pressure, $\text{Btu/lb } ^\circ\text{F}$
- D hydraulic diameter, ft
- f_c unit thermal convective conductance, $\text{Btu/hr ft}^2 ^\circ\text{F}$
- g gravitational force per unit of mass, $\text{lb}/(\text{lb sec}^2/\text{ft})$

- G weight rate per unit of area, lb/hr ft²
 G_a weight rate per unit of area for ventilating air, lb/hr ft²
 G_g weight rate per unit of area for exhaust gas, lb/hr ft²
 L length of heat transfer surface, ft
 P heat transfer perimeter, ft
 q_a measured rate of enthalpy change of ventilating air, Btu/hr
 q_g measured rate of enthalpy change of exhaust gas, Btu/hr
 t_1 arithmetic average temperature of heater surface at section defined by point 1, °F
 t_2 arithmetic average temperature of heater surface at section defined by point 2, °F
 T, T_a arithmetic average mixed mean absolute temperature of
 fluid = $\frac{T_1 + T_2}{2}$, °R
 T_1 mixed mean absolute temperature of fluid at point 1, °R
 T_2 mixed mean absolute temperature of fluid at point 2, °R
 T_{iso} mixed mean absolute temperature of fluid for isothermal pressure drop tests, °R
 U over-all unit thermal conductance, Btu/hr ft² °F
 W_a weight rate of air, lb/hr
 W_g weight rate of exhaust gas, lb/hr
 γ_1 weight density of fluid at entrance to heating section (point 1), lb/ft³
 ΔP non-isothermal pressure drop along heater, lb/ft²
 ΔP_a pressure drop along heater on ventilating air side, lb/ft²
 $\Delta P'_a$ pressure drop along heater on ventilating air side, inches H₂O

- ΔP_g pressure drop along heater on exhaust gas side, lb/ft²
- $\Delta P'_g$ pressure drop along heater on exhaust gas side, inches H₂O
- $\Delta P_{T_{iso}}$ isothermal pressure drop due to friction along heater at temperature T_{iso}
- Δt_{lm} logarithmic mean temperature difference, °F
- ΔT_a difference between mixed mean temperatures of ventilating air at sections defined by points 1 and 2,
 $= T_{a_2} - T_{a_1}$, °F
- ΔT_g difference between mixed mean temperatures of exhaust gas at sections defined by points 1 and 2,
 $= T_{g_1} - T_{g_2}$, °F
- T_{a_1} mixed mean temperature of ventilating air at section defined by point 1, °F
- T_{a_2} mixed mean temperature of ventilating air at section defined by point 2, °F
- T_{g_1} mixed mean temperature of exhaust gas at section defined by point 1, °F
- T_{g_2} mixed mean temperature of exhaust gas at section defined by point 2, °F

Point 1 refers to entrance end of heater.

Point 2 refers to exit end of heater.

DISCUSSION OF TEST RESULTS

Method of Analysis

(a) Heat transfer.— The thermal output of the heater was determined by the enthalpy change of the ventilating air:

$$q_a = W_a c_{pa} (T_{a_2} - T_{a_1}) \quad (1)$$

where c_{pa} was fixed (as a good approximation) at the arithmetic average air temperature. A plot of q_a against W_a with W_g as a parameter at approximately constant values of τ_{g_1} and τ_{a_1} is given in figures 17 and 21.

For the exhaust gas side:

$$q_g = W_g c_{pg} (\tau_{g_1} - \tau_{g_2}) \quad (2)$$

where c_{pg} was fixed (as a good approximation) at the arithmetic average exhaust gas temperature. The heat transfer to the surroundings was reduced to a negligible* rate as a result of wrapping with asbestos sheets.

The over-all thermal conductance UA was evaluated from the equation

$$q_a = (U A) \Delta t_m \quad (3)$$

Values of UA are plotted against W_a with W_g as a parameter in figures 18 and 22. Predicted values of UA were determined for both the Airesearch and Solar heaters, using the expression

$$UA = \frac{1}{\left(\frac{1}{f_{cP}}\right)_a \frac{1}{L} + \left(\frac{1}{f_{cP}}\right)_g \frac{1}{L}} \quad (4)$$

where the average thermal resistances for one foot of heater length $\left(\frac{1}{f_{cP}}\right)_a$ and $\left(\frac{1}{f_{cP}}\right)_g$, on the air and gas sides of the heater, respectively, are evaluated from chart B (see also reference 1); and L is the length of the heat transfer area. This nomographic chart is based on thermal data taken on smooth double tube heat exchangers in which the unit thermal conductance f_c can be expressed as:

$$f_c = 5.56 \times 10^{-4} \times T^{0.296} \frac{G^{0.80}}{D^{0.20}} \quad (5)$$

*Less than 3 percent on the exhaust gas side and less than 1 percent on the ventilating air side.

where T is the arithmetic average mixed mean absolute temperature of the fluid, G is the fluid flow per unit area, and D is the hydraulic diameter.

(b) Pressure drop.- The non-isothermal pressure drop of either fluid through the heater was predicted from isothermal pressure drop measurements by means of equation (27) of reference 1.*

$$\Delta P = \Delta P_{T_{\text{iso}}} \left(\frac{T_a}{T_{\text{iso}}} \right)^{1.13} + \frac{G^2}{(3600)^2 \gamma_i g} \left(\frac{T_2}{T_1} - 1 \right) \quad (6)$$

in which $\Delta P_{T_{\text{iso}}}$ is the isothermal pressure drop due to friction at temperature T_{iso} . A comparison of the measured and predicted magnitudes of the non-isothermal pressure drops is shown in figures 19, 20, 23, and 24.

Results on Airesarch Heat Exchanger Tests

The enthalpy change of the ventilating air was used as the criterion for the determination of the thermal output of the heat exchanger, since the temperature measurements on the air side are more accurate. A 1 percent error in the measurement of either exhaust gas temperature could cause a 10 percent error in the magnitude of the temperature change of the gas so that the heat balances are sometimes as much as 40 percent unbalanced. The average discrepancy in the heat balances q_g/q_a for these tests was 20 percent.

In figure 18 the values of the over-all conductance UA derived from laboratory measurements are compared with the values predicted by means of equation (4) and chart B, of reference 1, which is included with this report for convenience. The exchanger length L was taken to be $21\frac{1}{2}$ inches, which is the sum of the full-fluted heat transfer length (17 in.) and one-half of each tapered end section ($4\frac{1}{2}$ in.). The choice of this length is somewhat arbitrary, since the mechanism and rate of heat transfer at the ends of the heater is complicated by the cross-flow and tapered characteristics of the inlet and outlet ventilating air ducts and the tapered fluted heater ends. The prediction as given herein is, however, a conservative one. The predicted values are within 18 percent of the measured values. The fact that the latter data do not fall on truly continuous curves can be explained in part by the experimental errors in determining the log mean temperature differences.

* T_{iso} is substituted for T_1 in the first term on the right-hand side of equation (27) of reference 1. In reference 1, T_1 coincided with T_{iso} , but this was not the case in these tests, especially on the exhaust gas side.

The predicted non-isothermal pressure drops calculated from the measured isothermal pressure drops compare well with the measured non-isothermal values, as shown in figures 19 and 20.

The temperatures of the heater surfaces are probably slightly low due to conduction of heat along the porcelain-insulated thermocouple wires which extended through the ventilating air stream.

The thermal and pressure-drop data obtained in the tests of the Airesearch heat exchanger are contained in tables I and II. Corresponding data from the tests made on the Solar heat exchanger are included in tables III and IV.

Results on Solar Heat Exchanger Tests

Because, during the tests on the Solar heater a part of the mixing chamber became disengaged, the single measurement of the exhaust gas temperature at the center of the duct was inadequate for the determination of the mixed mean temperature at the entrance to the heater. Previous to the disengaging of the mixing chamber the exhaust gas inlet temperature was quite uniform. The marked change in the heat balance ratio q_g/q_a (see table III), is traceable to this fact. For runs numbers 17 to 24 the exhaust gas temperature T_{g_1} was calculated from T_{g_2} and the equation $q_g = q_a$ in order to determine the over-all conductance UA and to calculate the non-isothermal pressure drop correction.

In figure 22 the values of the over-all conductance UA determined from laboratory measurements are compared with the values predicted by means of equation (4) and chart B of reference 1. The heat transfer length L was taken to be $15\frac{1}{2}$ inches, which is the sum of the full-fluted length (11 inches) and one-half of each tapered end section ($4\frac{1}{4}$ inches). As in the prediction of the previous heater the choice of this length was somewhat arbitrary but is one which yields a conservative value of the over-all thermal conductance. The predicted values of UA are up to 20 percent lower than those derived from the measurements.

Because it was not possible to install the static pressure taps on the exhaust gas side immediately before and after the heating section owing to the presence of the close-fitting air shroud, the measured isothermal pressure drop $\Delta P_{T_{iso}}$ was more than that due to

friction alone - that is, it included expansion and contraction losses. However, only the isothermal pressure drop due to friction should be substituted for $P_{T_{iso}}$ and multiplied by $\left(\frac{T_a}{T_{iso}}\right)^{1.13}$

in equation (6). The expansion and contraction losses included in the measured value of $\Delta P_{T_{iso}}$ are not the same function of the fluid temperatures as the losses due to friction; thus the predicted magnitude of the non-isothermal pressure drop is slightly in error. (See fig. 23.)

On the ventilating air side of the Solar heater the greater portion of the pressure drop occurred in the converging and diverging sections placed before and after the heated section; so the above-mentioned calculation was not at all accurate.

When the pressure drops due to causes other than friction are accurately calculated and subtracted from the total measured isothermal pressure drop, the additional pressure drop due to the heating of the fluid can be predicted from equation (6). If the variation of the expansion and contraction losses with fluid temperature is known, the total non-isothermal pressure drop can be calculated.

At a ventilating air flow of about 3000 pounds per hour the velocity distribution of the air around the periphery of the Solar air shroud at the entrance to the heater section was uniform for about 60 percent of the perimeter. Along one portion of the shroud the velocity diminished. However, at a ventilating air rate of 6000 pounds per hour the velocity distribution was uniform (± 10 percent) around the entire shroud.

The measurements of surface temperatures are considered to be slightly low due to conduction of heat along the porcelain-insulated thermocouple wires.

Comparison of Airesearch and Solar Heat Exchanger Performance

The average thermal resistances $\left(\frac{1}{f_c A}\right)_a$ and $\left(\frac{1}{f_c A}\right)_g$

for the air and gas sides, respectively, are equal as determined from chart B of reference 1 at a ratio of exhaust gas flow to ventilating air flow approximately equal to 1.2 for the Airesearch

heater and 1.4 for the Solar heater. These results indicate a proper distribution of thermal resistance for the optimum rate of heat transfer at a usual operating flow ratio. However, in some heaters it may be advantageous to proportion the thermal resistances in order to yield a safe operating temperature of the heater metal.

The heat transfer rate for the Airesearch heater is about 85 percent greater than that for the Solar unit mainly because of the larger heat transfer area of the former (ratio of areas, 2.25:1).

At an exhaust gas flow of 7000 pounds per hour and a ventilating air flow of 5000 pounds per hour the thermal output of the Airesearch heater was about 320,000 Btu per hour and that of the Solar was approximately 170,000 Btu per hour (ratio = 1.9). At these same weight rates the non-isothermal pressure drop on the air side was 50 percent greater and on the gas side 25 percent greater for the Airesearch than for the Solar unit. The isothermal pressure drop for both the air and gas sides was about 33 percent greater for the Airesearch heater than for the Solar heater. A satisfactory correlation of the pressure drop and heat transfer results should not be expected, especially on the air side of these heaters, because of the inclusion of inlet and outlet duct pressure drops.

It may be seen from figures 17, 18, 21, and 22 that the change in the thermal output q_a and the corresponding over-all thermal conductance UA with increasing gas and air rates is greater for the Airesearch heater than for the Solar heater. For fixed magnitudes of gas and air weight rates the corresponding weight rates per unit area G are larger in the case of the Solar heater since the cross-sectional areas on the air and gas sides are smaller. Since the unit thermal conductances f_c on both sides of the heaters are functions of the 0.8 power of G , the increase in the magnitude of f_c with an increase in G is less at higher values of G - that is, $f_c \propto G^{0.8}$; so

$$\frac{df_c}{dG} \propto \frac{1}{G^{0.2}} .$$

CONCLUSIONS

1. At an exhaust gas flow rate of 7000 pounds per hour

and a ventilating air flow rate of 5000 pounds per hour, the thermal output of the Airesearch heat exchanger was about 320,000 Btu per hour, while that of the Solar unit was about 170,000 Btu per hour. The heat transfer area of the Airesearch heat exchanger is about 2.25 times as great as that of the Solar heater, and this difference largely accounts for the greater thermal output of the Airesearch heat exchanger.

2. The thermal performance of the Airesearch and Solar fluted-type heat exchangers can be estimated to within 20 percent by use of equations (3) and (4), and equation (5) which is based on the unit thermal conductance, for smooth tubes.

3. The non-isothermal pressure drop due to friction can be closely estimated from isothermal values measured across the heating section.

4. Within the usual operating range of flow ratios, the thermal resistances on the gas and air sides of both heaters previously mentioned are evenly proportioned.

University of California,
Berkeley, Calif.

REFERENCES

1. Martinelli, R. C., Weinberg, E. B., Morrin, E. H., and Boelter, L. M. K.: An Investigation of Aircraft Heaters. III - Measured and Predicted Performance of Double Tube Heat Exchangers. NACA A.R.R. Oct. 1942.
2. Anon.: Fluid Meters, Their Theory and Application. A.S.M.E. Res. Pub., 4th ed., Pt. I, 1937.
3. King, W. J.: Measurement of High Temperatures in High-Velocity Gas Streams. A.S.M.E. Trans., vol. 65, No. 5, July 1943, pp. 421-428; discussion, pp. 428-431.

TABLE I
AIRESEARCH FLUTED-TYPE HEATER

Run No.	Air Side					Exhaust Gas Side					$\frac{q_g}{q_a}$	Heater Temperatures			Pressure Drops			Overall Performance	
	T_{a1}	T_{a2}	ΔT_a	W_a	q_a	T_{g1}	T_{g2}	ΔT_g	W_g	q_g		t_1	t_2	t_f	ΔP_a	ΔP_g	ΔP_f	ΔT_m	(UA)
	°F	°F	°F	lbs/hr	Btu/hr	°F	°F	°F	lbs/hr	Btu/hr		°F	°F	°F	Inch. H ₂ O	Inch. H ₂ O	ft. H ₂ O	°F	Btu/hr/ft ² of
10	104	362	258	4280	266,000	1455	1332	123	4200	142,000	359	562	15.4	2.75	1150	231			
11	104	323	219	5100	270,000	1446	1287	159	4200	184,000	327	508	20.5	2.75	1140	237			
12	104	310	206	5680	286,000	1446	1282	164	4200	190,000	306	478	23.6	2.75	1150	249			
13	104	337	233	5450	308,000	1407	1275	132	6055	220,000	352	537	23.2	5.15	1105	279			
14	99	352	253	5080	311,000	1407	1279	128	6055	214,000	365	545	20.5	5.20	1115	279			
15	104	368	264	4380	280,000	1407	1282	125	6055	208,000	386	559	16.0	5.25	1110	252			
16	99	426	327	3080	244,000	1390	1298	92	6055	153,000	460	645	8.65	5.35	1070	228			
17	96	437	341	3080	254,000	1441	1302	139	7285	279,000	488	723	8.90	8.00	1105	230			
18	96	384	288	4400	306,000	1441	1296	145	7280	291,000	413	628	16.4	7.60	1140	268			
19	96	362	266	5100	328,000	1441	1286	155	7280	310,000	386	594	21.1	7.70	1155	284			
20	102	357	255	5420	334,000	1460	1302	158	7280	316,000	382	580	23.2	7.65	1180	283			
21	99	375	276	5420	362,000	1441	1279	162	8650	385,000	410	572	23.5	10.5	1140	318			
22	97	386	289	5010	352,000	1441	1288	153	8650	364,000	427	580	20.9	10.6	1130	312			
23	96	410	314	4380	334,000	1441	1277	164	8700	392,000	453	603	16.6	10.8	1120	298			
24	99	457	358	3180	275,000	1372	1270	102	8750	246,000	517	676	9.50	11.0	1030	267			

^aArithmetic average of three surface temperatures measured near exhaust gas inlet to heater

^bArithmetic average of three surface temperatures measured near exhaust gas outlet to heater

AIRESEARCH FLUTED-TYPE HEATER

Pressure Drop Data

Run No.	W lbs/hr	G lbs/hr ft ²	Measured isothermal pressure drop ^a $\Delta P_{T_{iso}}$ lbs/ft ² ($T_{iso}=560^{\circ}R$)	Predicted non-isothermal pressure drop ΔP lbs/ft ²	Measured non-isothermal pressure drop ΔP lbs/ft ²	T ₁ °R	T ₂ °R	T _a °R
Air Side								
16	3080	17,980	31.5	48.5	45.9	559	886	722
10	4280	24,900	57.0	81.7	80.0	564	822	693
19	5100	29,700	79.0	112.0	109.5	556	822	689
20	5420	31,600	88.5	125.5	120.2	562	817	689
Exhaust Gas Side								
10	4203	15,600	4.60	15.2	14.3	1915	1792	1853
16	6055	22,500	8.96	30.8	27.8	1856	1758	1807
19	7280	27,000	12.30	38.7	40.0	1901	1746	1823
20	8650	32,100	16.60	54.0	55.0	1901	1748	1824

^a These entries are taken from plot of ΔP_a vs. W_a
or ΔP_g vs. W_g since actual isothermal measurements were
at slightly different fluid rates.

$$\Delta P = \Delta P_{T_{iso}} \left(\frac{T_a}{T_{iso}} \right)^{1.13} + \frac{G^2}{(3600)^2 \cdot \gamma \cdot g} \left(\frac{T_2}{T_1} - 1 \right) \quad (6)$$

TABLE III
SOLAR FLUTED-TYPE HEATER

Run No.	Air Side				Exhaust Gas Side				$\frac{q_g}{q_a}$	Heater Temperatures			Pressure Drop			Overall Performance	
	T_{a1}	T_{a2}	ΔT_a	W_a	q_a	T_{g1}	ΔT_g	W_g		q_g	t_1	t_2	ΔP_g	ΔP_g	ΔT_{gm}	(UA)	
	$^{\circ}F$	$^{\circ}F$	$^{\circ}F$	lbs/hr	Btu/hr	$^{\circ}F$	$^{\circ}F$	lbs/hr		Btu/hr	$^{\circ}F$	$^{\circ}F$	Inch. H ₂ O	Inch. H ₂ O	$^{\circ}F$	Btu/hr/ft ² oF	
9	99	276	177	3020	130,000	1394	1325	5200	99,000	0.76	445	6.1	5.80	3.30	1160	112	
10	96	231	135	4320	141,000	1360	1282	5195	111,000	0.79	353	498	10.4	3.05	1155	122	
11	96	210	114	5340	147,000	1372	1286	5195	123,000	0.83	318	438	15.2	3.05	1180	124	
12	97	207	108	6350	166,000	1377	1295	5105	115,000	0.69	293	408	18.7	3.00	1190	139	
13	95	215	120	6350	184,000	1351	1273	6520	140,000	0.76	321	532	18.7	4.95	1160	159	
14	98	227	129	5300	166,000	1356	1282	6620	135,000	0.81	365	576	15.0	5.00	1160	143	
15	95	251	156	4310	163,000	1390	1316	6620	135,000	0.83	417	650	10.5	5.20	1180	138	
16	97	290	193	3050	142,000	1390	1316	6620	135,000	0.95	489	740	5.70	5.40	1155	123	
17	100	284	184	3110	138,000	1448	1338	7600	230,000	1.66	581	770	5.90	7.45	1185	117	
18	99	254	155	4300	161,000	1525	1329	7820	422,000	2.62	424	650	10.2	7.30	1195	135	
19	97	236	137	5300	176,000	1569	1351	7740	464,000	2.63	386	598	15.0	7.15	1210	145	
20	95	224	129	6200	194,000	1553	1329	7740	477,000	2.46	352	554	18.2	7.00	1210	160	
21	94	222	128	6200	192,000	1525	1290	8440	545,000	2.84	359	550	17.5	8.00	1180	163	
22	96	230	134	5300	172,000	1481	1273	8490	485,000	2.82	384	572	14.3	8.20	1120	154	
23	95	265	170	4300	177,000	1503	1299	8340	468,000	2.64	473	671	9.85	7.95	1160	152	
24	97	301	204	3050	151,000	1486	1303	8290	418,000	2.78	553	761	5.45	7.95	1130	133	

a T_g for runs 17-24 is in error because of mixing chamber failure
 b See footnote at bottom of Table I
 c For runs 13-24 two temperature measurements were made near exit end.
 d T_g was derived from T_{g1} and $q_a = q_g$ in order to evaluate ΔT_{gm} for runs 17-24

SOLAR FLUTED TYPE HEATER

Pressure Drop Data

Run No.	W_g lbs/hr	G_g lbs/hr/ft ²	Measured isothermal pressure drop ^a $\Delta P_{T_{iso}}$ lbs/ft ² ($T_{iso}=556^\circ R$)	Predicted non-isothermal pressure drop ΔP lbs/ft ²	Measured non-isothermal pressure drop ΔP lbs/ft ²	T_1^b °R	T_2 °R	T_a °R
Exhaust Gas Side								
10	5190	26,700	5.2	15.7	15.8	1820	1742	1781
14	6620	34,100	8.0	23.7	26.0	1816	1742	1779
20	7740	39,500	10.5	31.1	36.1	1880	1789	1835
22	8500	43,800	12.3	37.8	42.6	1807	1733	1770
Air Side								
	W_a lbs/hr	G_a lbs/hr/ft ²	($T_{iso}=560^\circ R$)					
1	3200	35,500	25.2	--	--	--	--	--
2	4300	47,800	44.9	--	--	--	--	--
3	5330	59,300	67.0	--	--	--	--	--
4	6350	70,700	90.0	--	--	--	--	--
9	3020	33,600	--	--	30.2	559	736	657
15	4310	47,900	--	--	54.3	555	711	633
19	5300	58,800	--	--	77.6	557	696	626
12	6350	70,500	--	--	97.0	557	667	612

^a The entries are taken from plot of ΔP vs. W_g since actual isothermal measurements were at slightly different gas rates.

^b T_1 evaluated from T_2 and $q_a = q_g$ for runs 20 and 22.

$$\Delta P = \Delta P_{T_{iso}} \left(\frac{T_a}{T_{iso}} \right)^{1.13} + \frac{G^2}{(3600)^2 \gamma g} \left(\frac{T_2}{T_1} - 1 \right) \quad (6)$$

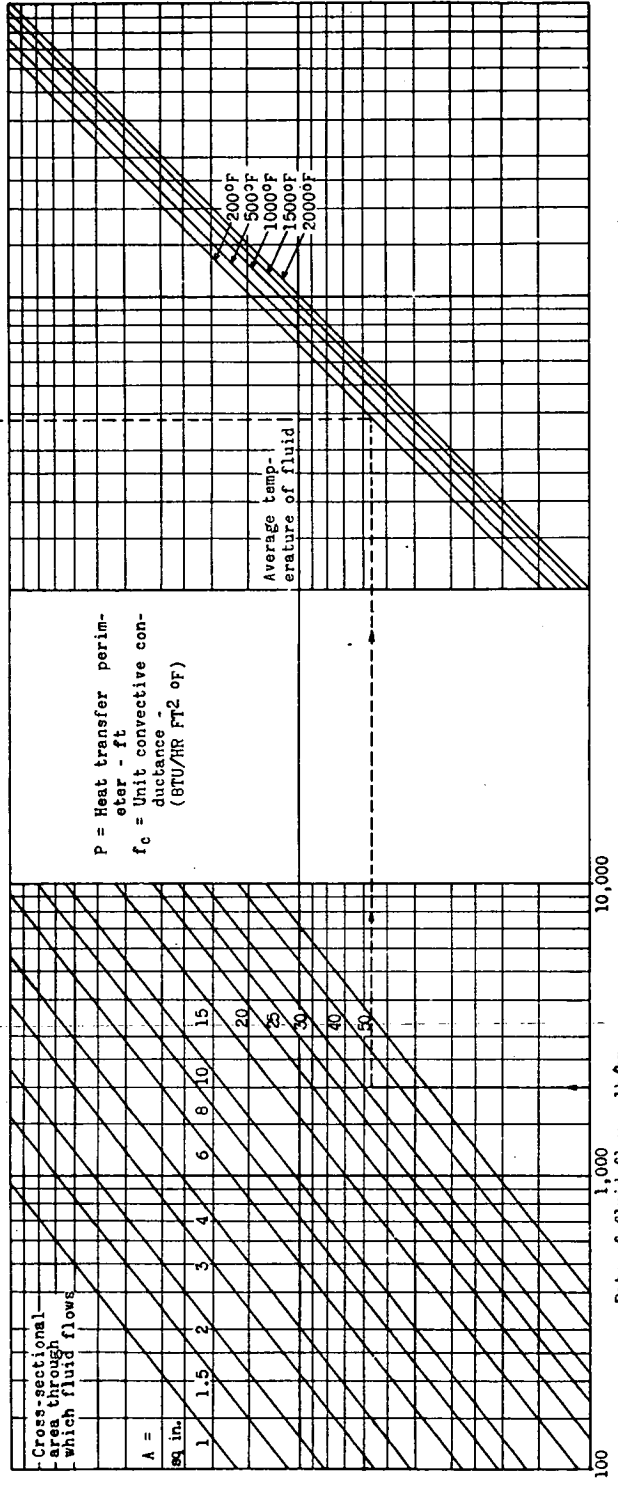
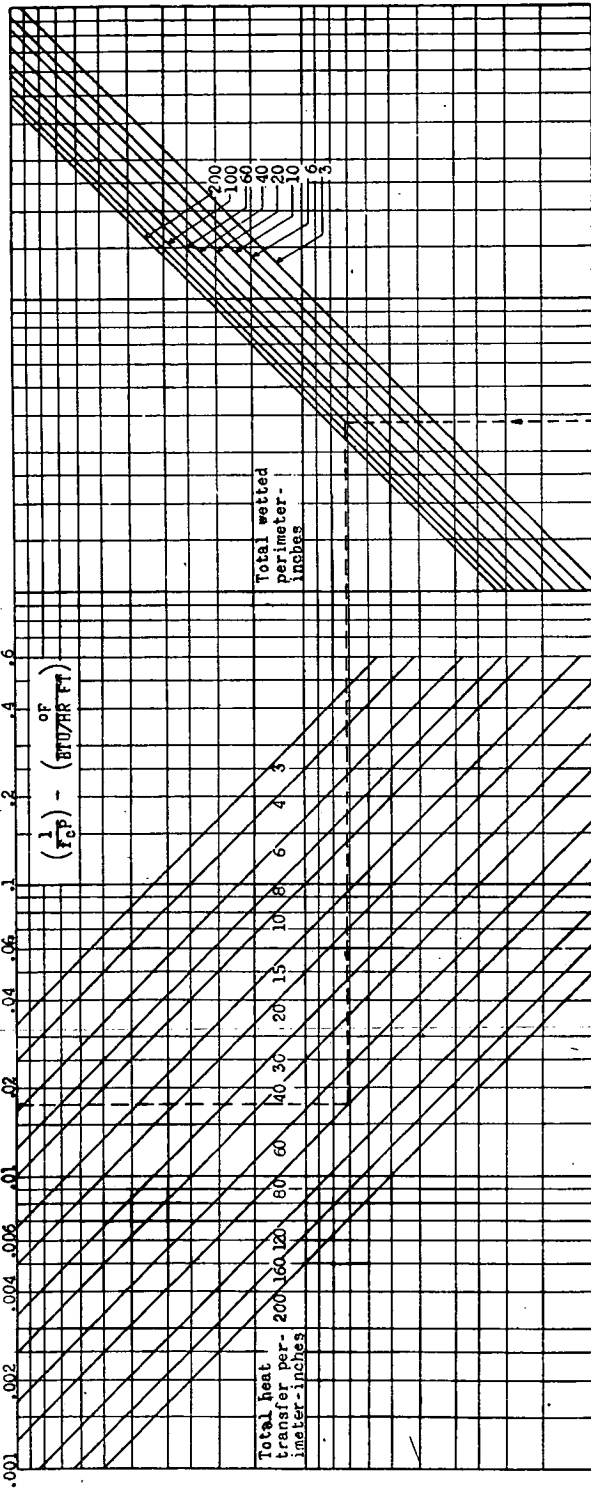
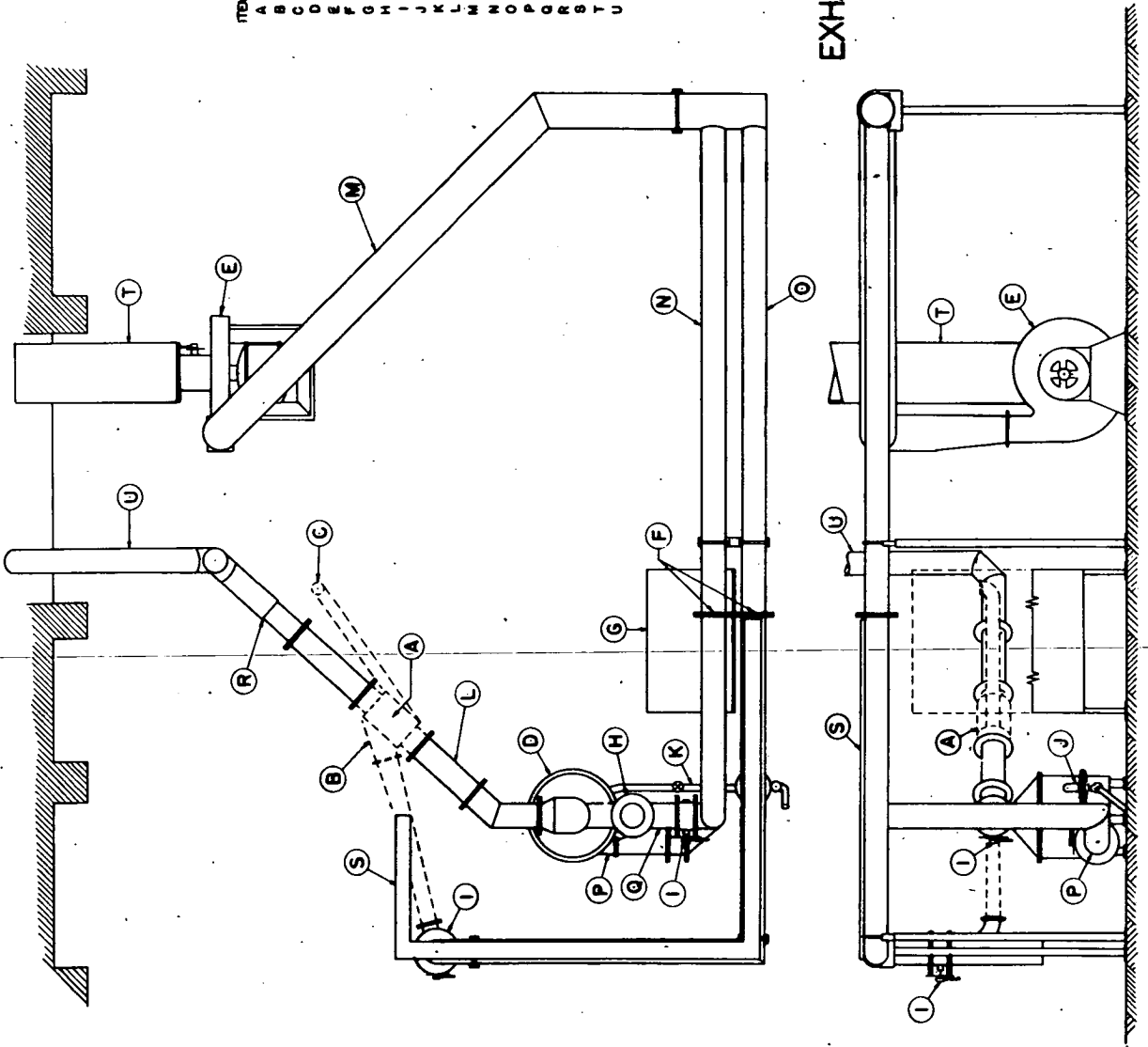


Chart B

- | ITEM | DESCRIPTION |
|------|--------------------------------|
| A | HEATER |
| B | TYPICAL VENTILATING AIR SHROUD |
| C | VENTILATING OUTLET |
| D | FURNACE - BESLER MODEL |
| E | BLOWER |
| F | CRIFICE |
| G | INSTRUMENT STATION |
| H | SAFETY VALVE |
| I | BUTTERFLY VALVES |
| J | PRESSURE REGULATING VALVE |
| K | GAS LINE |
| L | MIXING SECTION |
| M | BLOWER OUTLET |
| N | COMBUSTION AIR 12" PIPE |
| O | VENTILATING AIR 8" PIPE |
| P | COMBUSTION AIR TO BURNER |
| Q | EXHAUST AIR TO BURNER |
| R | EXHAUST GAS COOLING AIR |
| S | EXPANSION JOINT |
| T | THERMOCOUPLE CONDUIT |
| U | AIR INTAKE DUCT |
| V | EXHAUST GAS OUTLET |

FIGURE 1.
EXHAUST GAS-AIR HEATER
TEST STAND



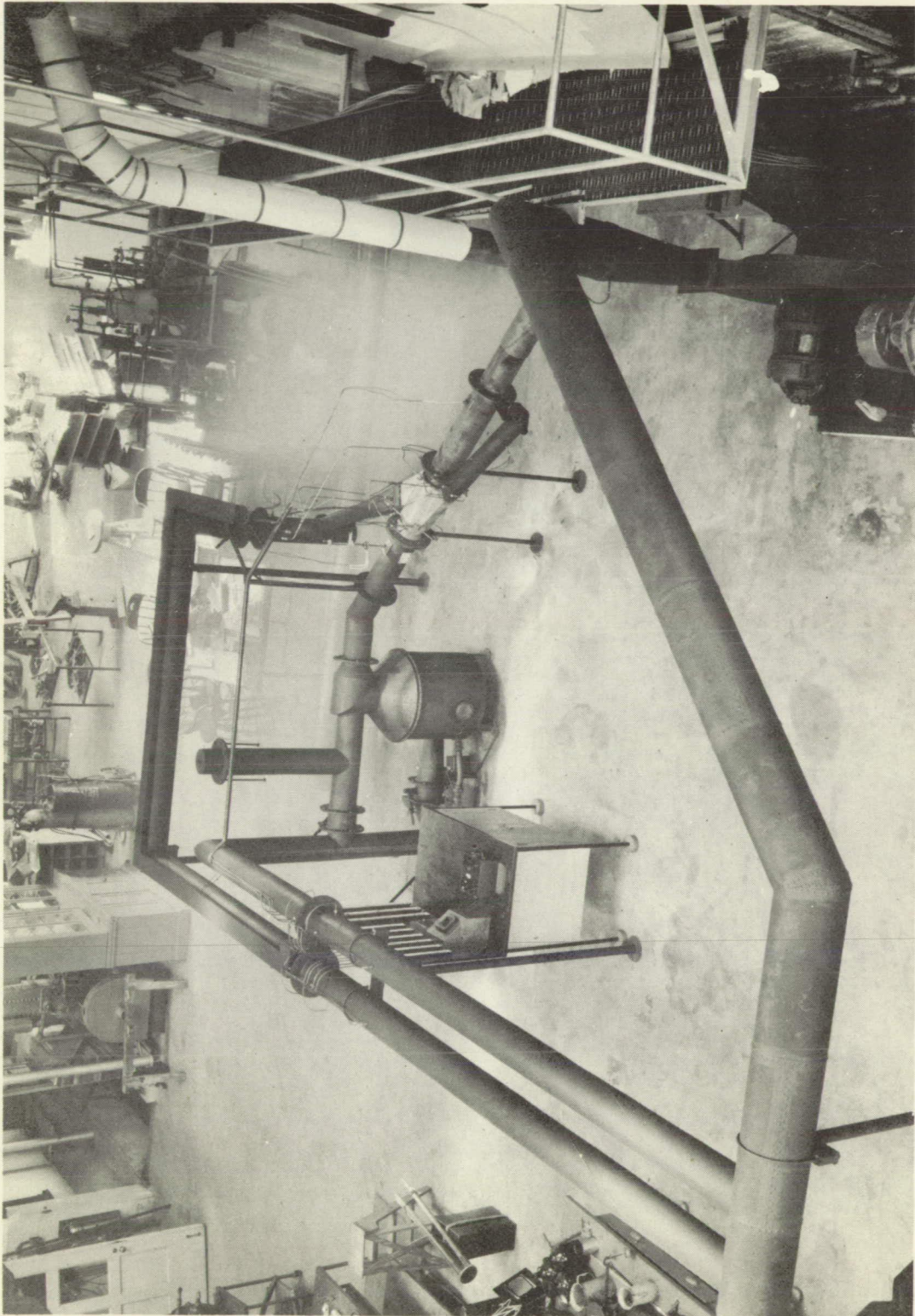


Figure 2.- Photograph of heater test stand.

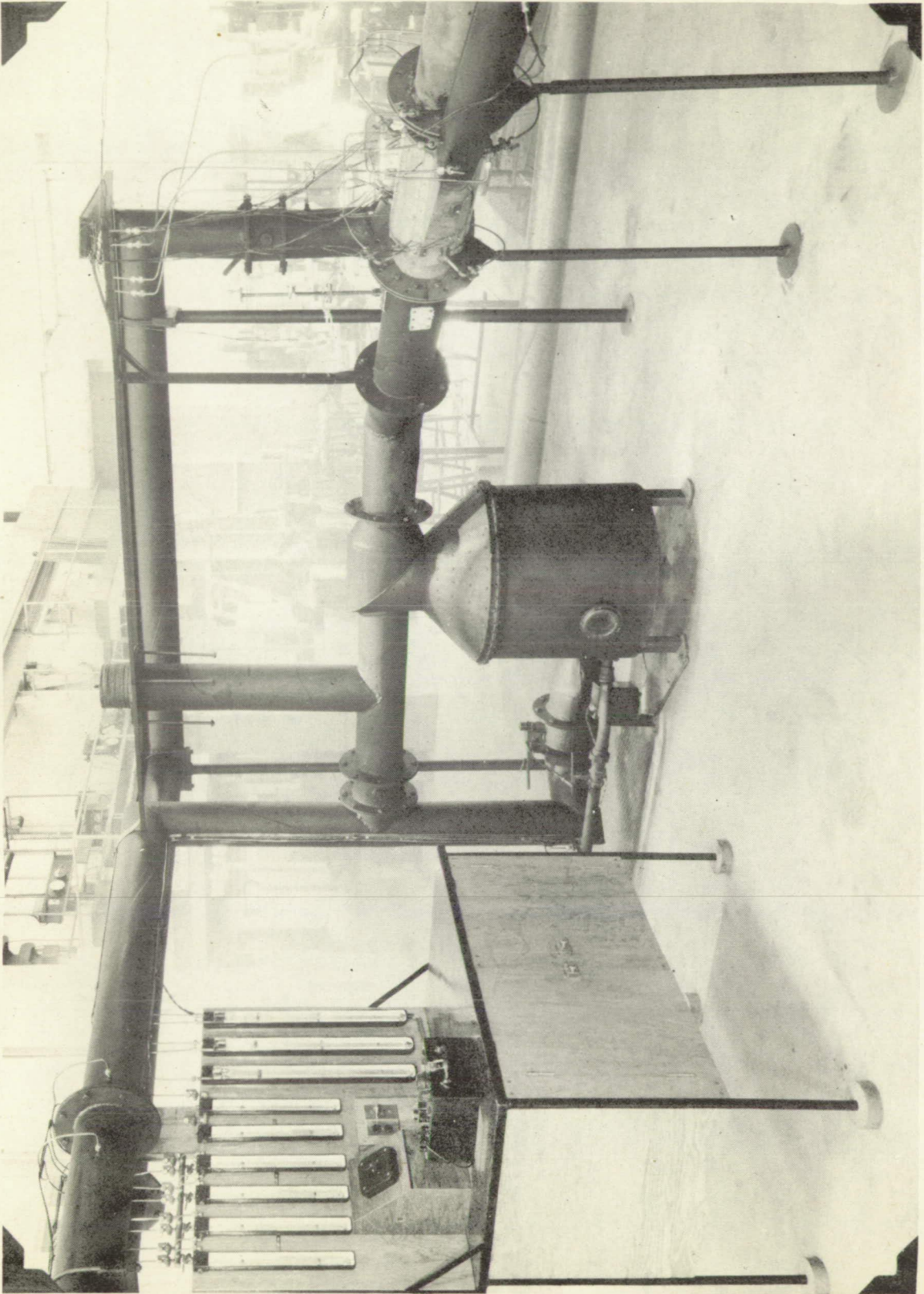


Figure 3.- Photograph of data station, furnace and heater section.

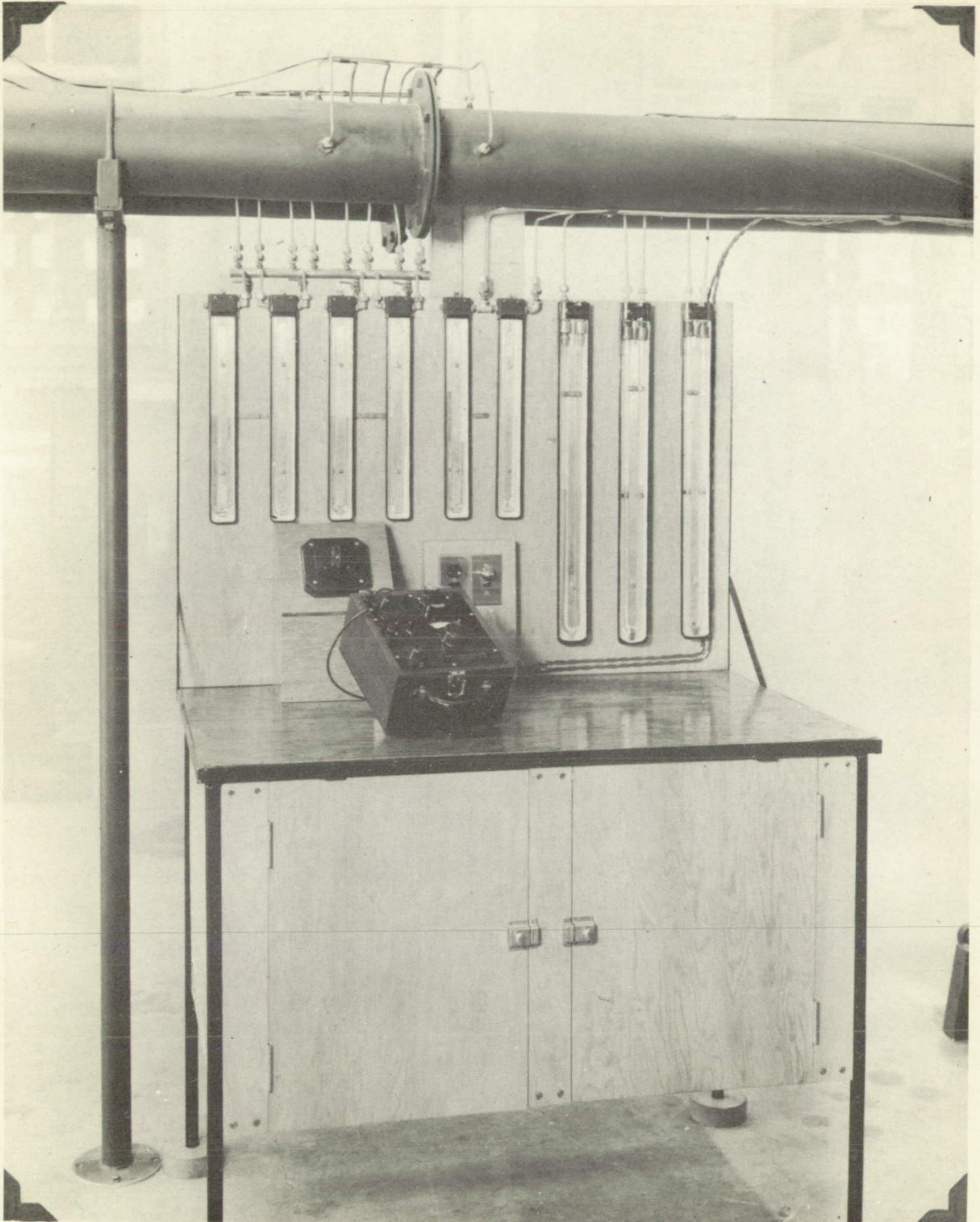


Figure 4.- Photograph of data station and orifice meters.

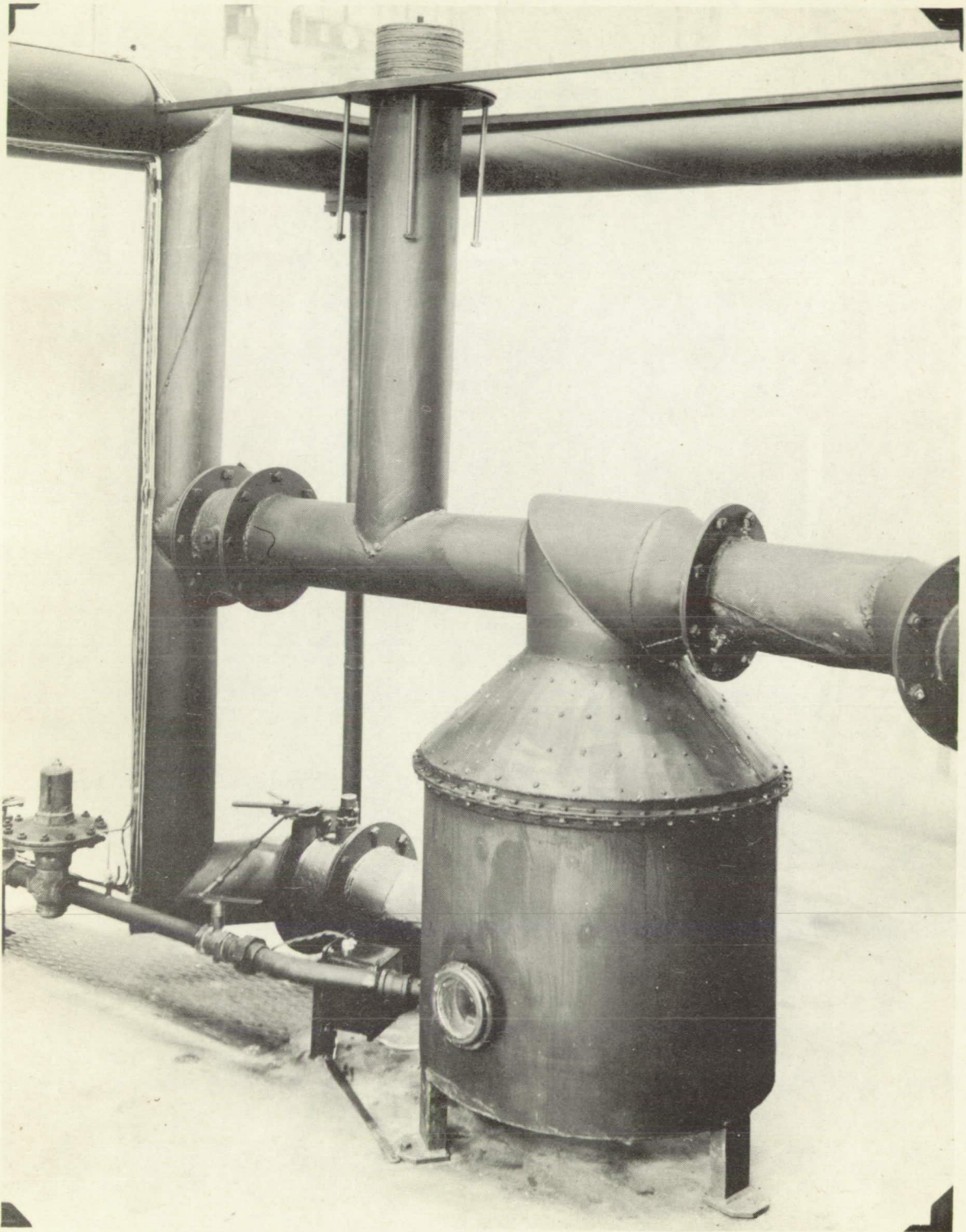


Figure 5.- Photograph of natural gas furnace.

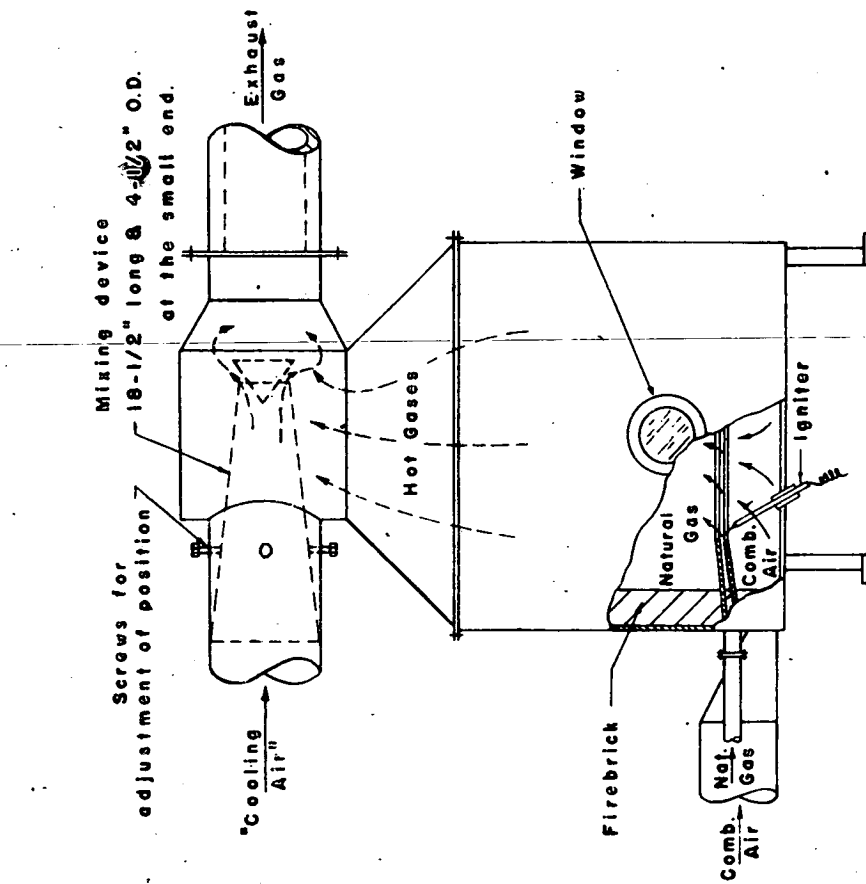


Fig. 6.- Sketch of Furnace Showing Mixing Device.

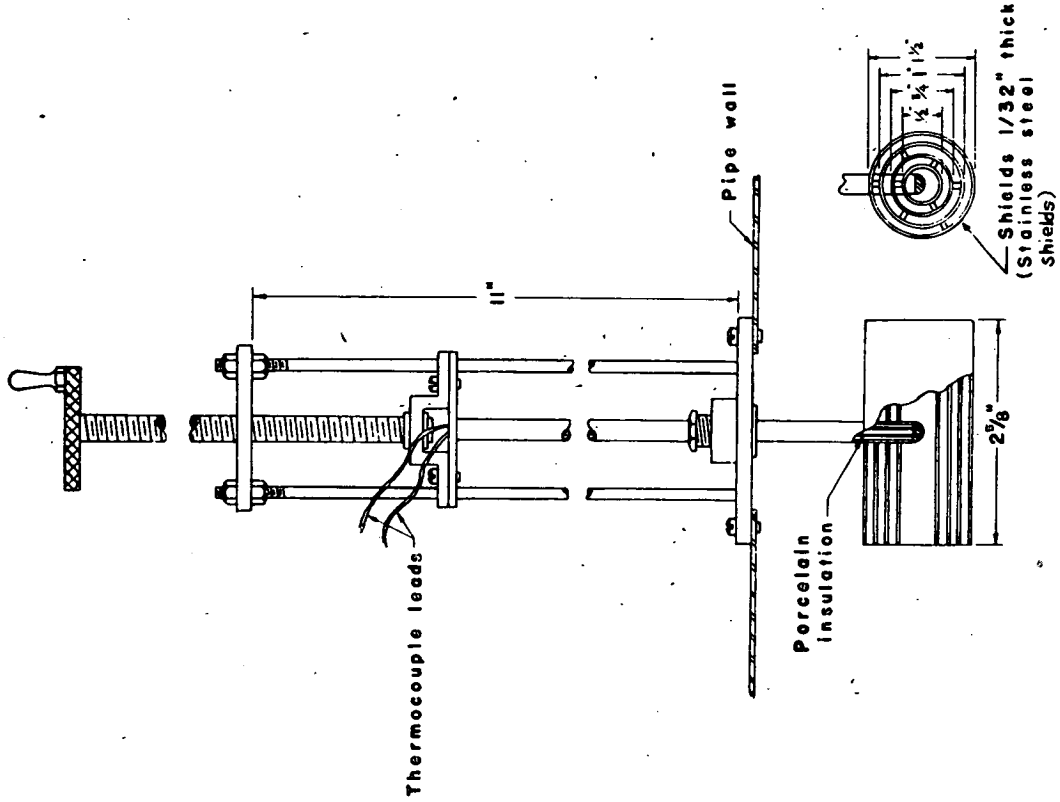


Fig. 8.- Sketch of Shielded Traversing Thermocouple.

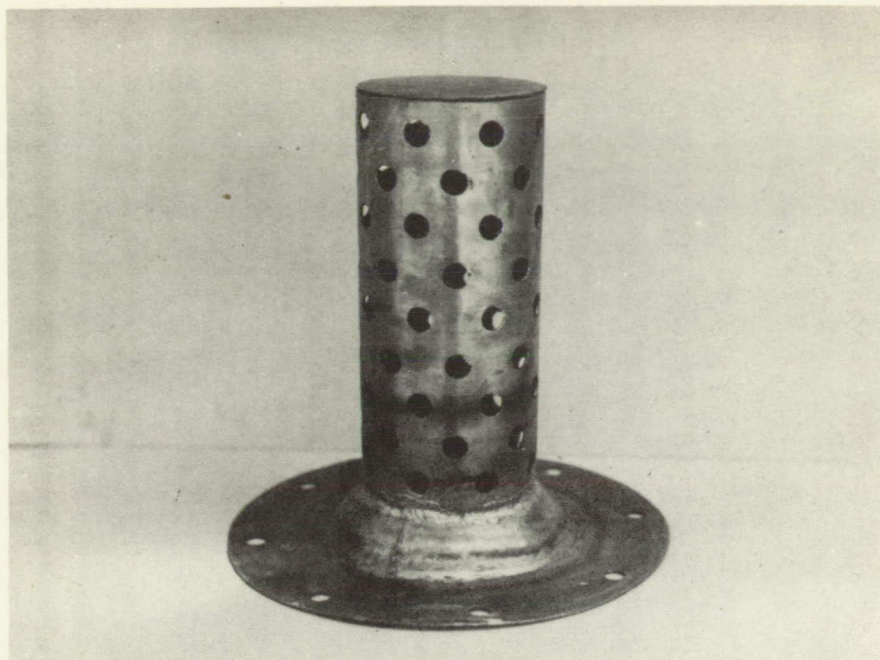


Figure 7.- Photograph of a mixing device.

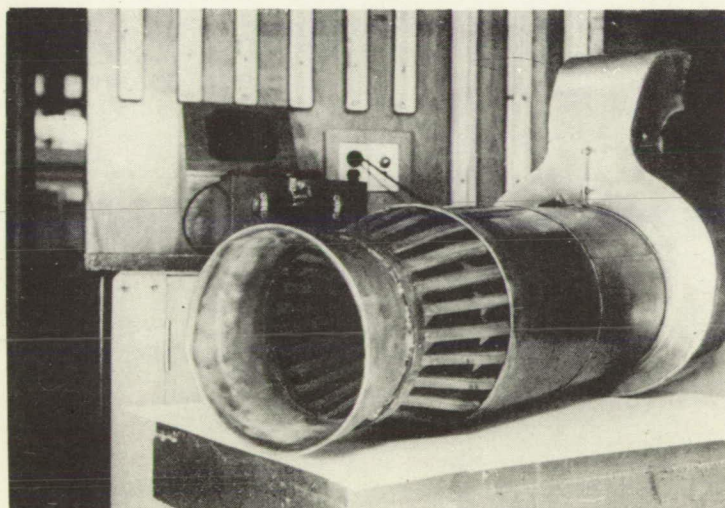
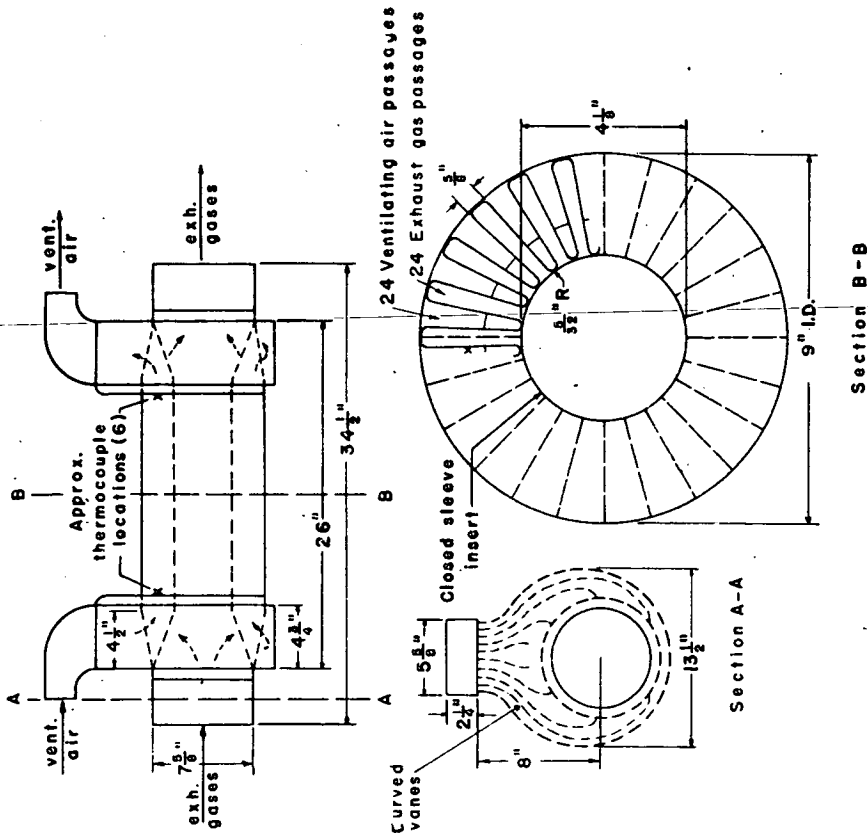
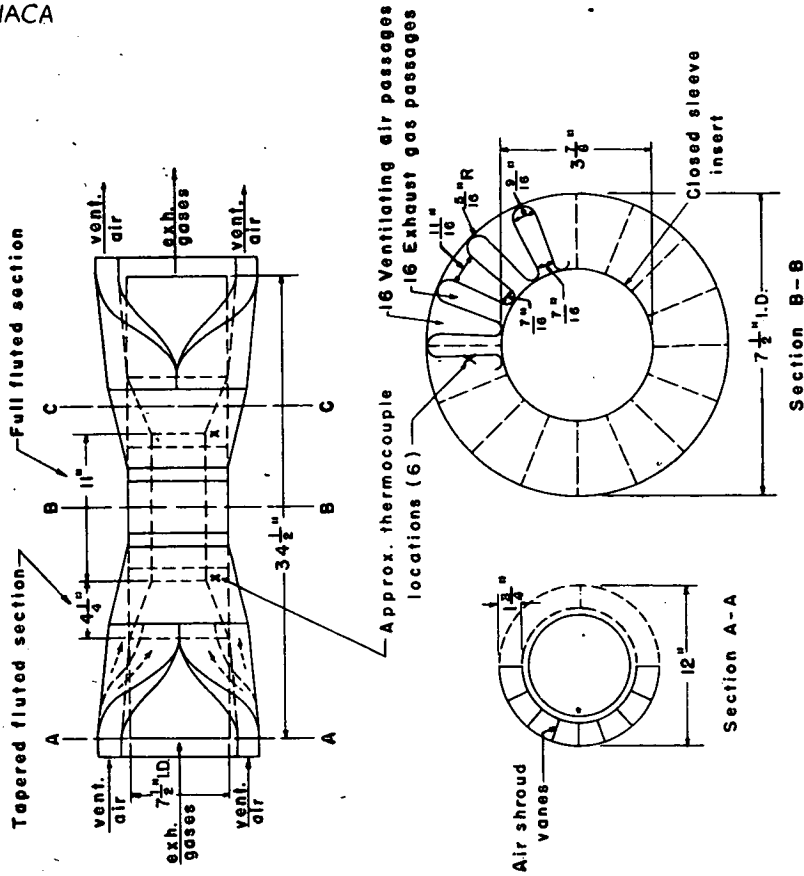


Figure 10.- Photograph of Airesearch heater and air shroud with outlet header removed.



	Section B-B	Air	Gas
Gross section area, ft. ²		0.172	0.270
Wetted perimeter, ft.		12.9	13.3
Heat transfer perimeter, ft.		10.1	10.1
Weight of heater - Shroud		38 1/4 lbs.	10 1/2 lbs.

Fig. 9.- Schematic Diagram of Air Research Heater and Air Shroud.



	Sect. B-B	Air	Gas
Gross section area, ft. ²		0.112	0.194
Wetted perimeter, ft.		7.60	7.68
Heat transfer perimeter, ft.		5.66	5.66
Weight of heater - Shroud		19 1/4 lbs.	7 1/4 lbs.

Fig. 13.- Schematic Diagram of Solar Heater and Air Shroud

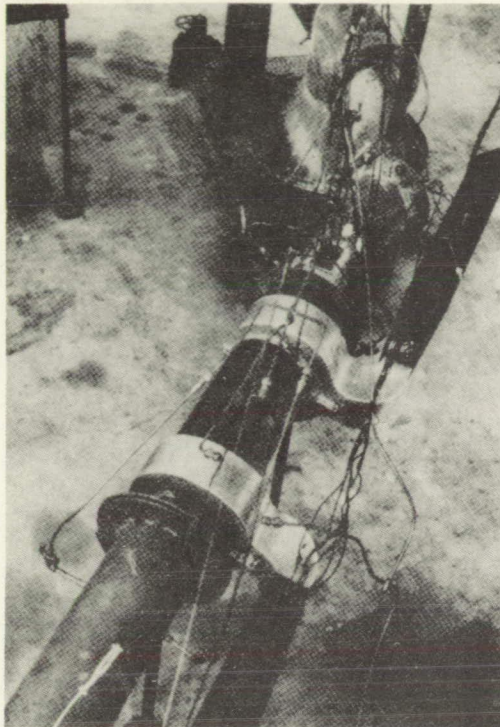


Figure 11.- Photograph of Airesearch heater in test stand.

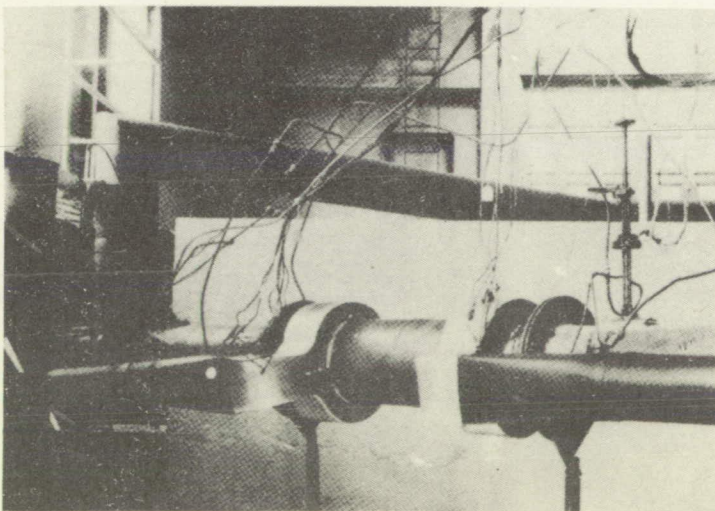


Figure 12.- Photograph of Airesearch heater in test stand.

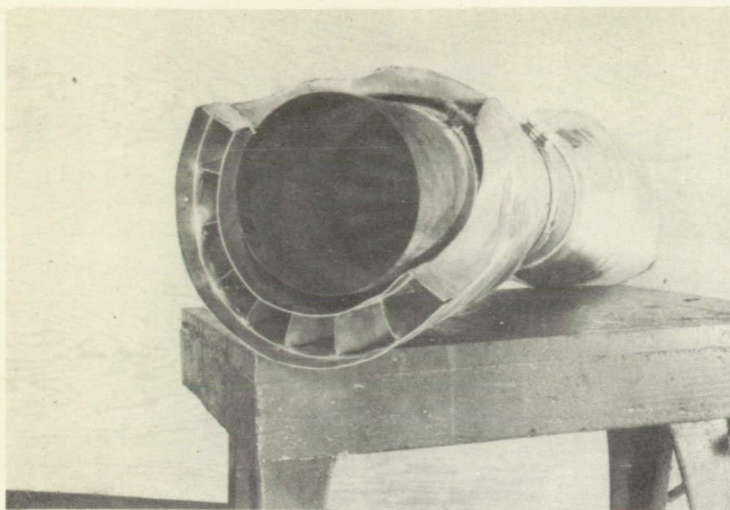


Figure 14.-
Photograph
of Solar
heater
and air
shroud.

Figure 15.-
Photograph
of Solar
heater
in test
stand.

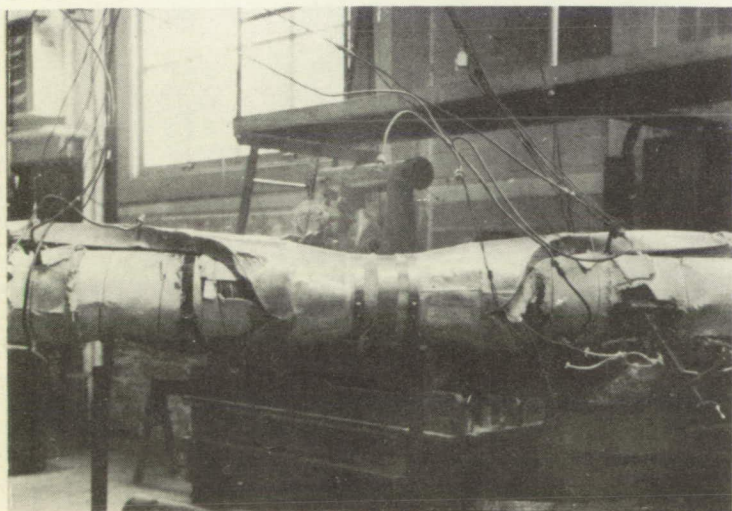
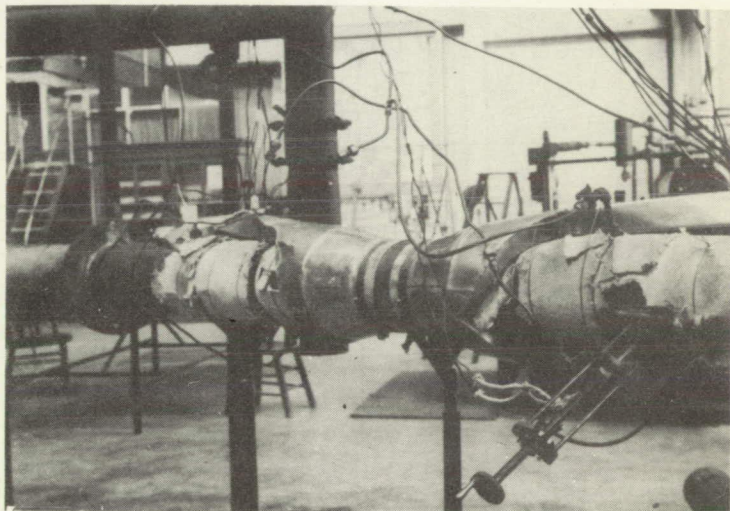


Figure 16.-
Photograph
of Solar
heater
in test
stand.

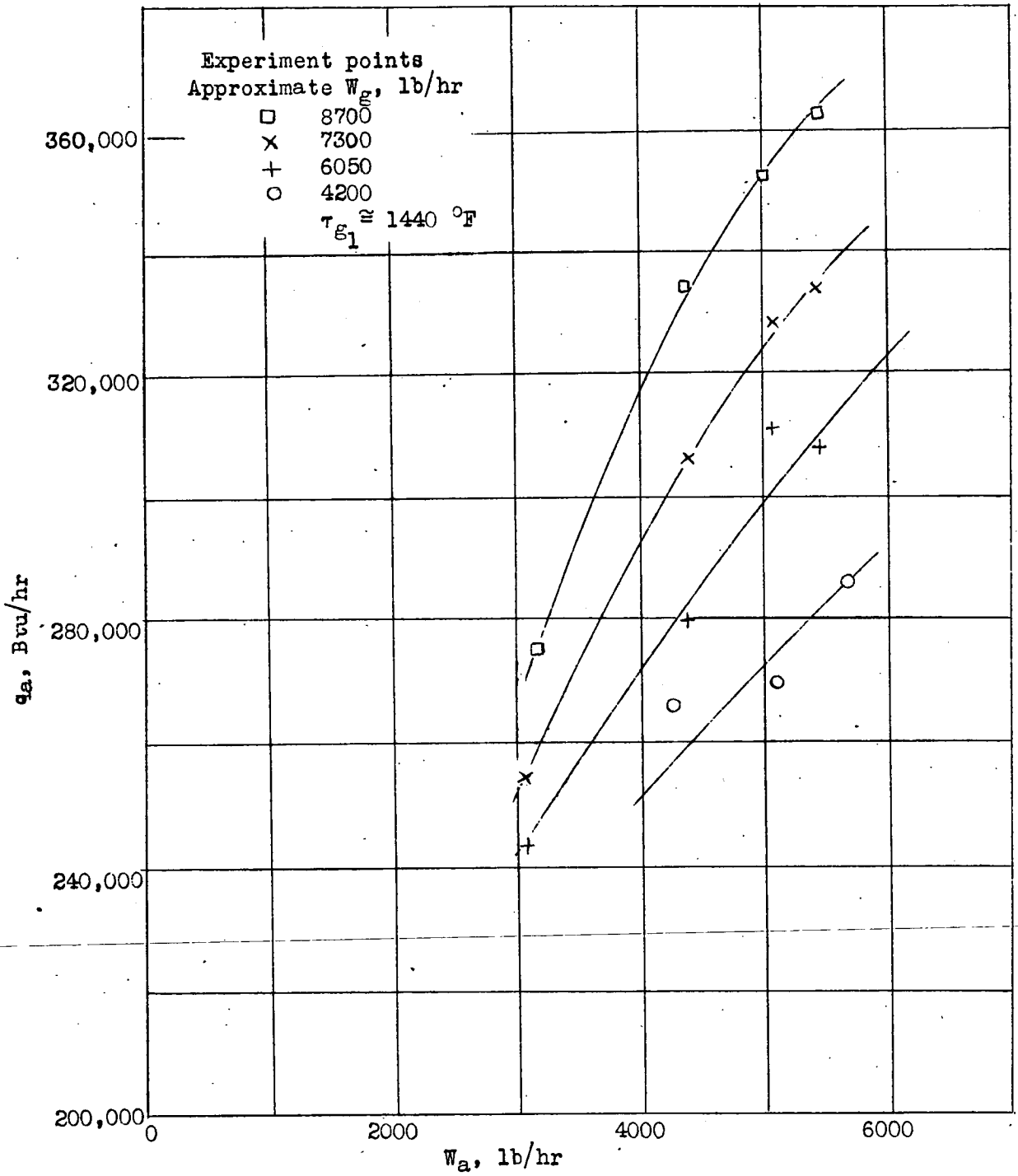


Figure 17.- Thermal output of Airesearch fluted type exhaust gas-air heat exchanger as a function of the ventilating air rate.

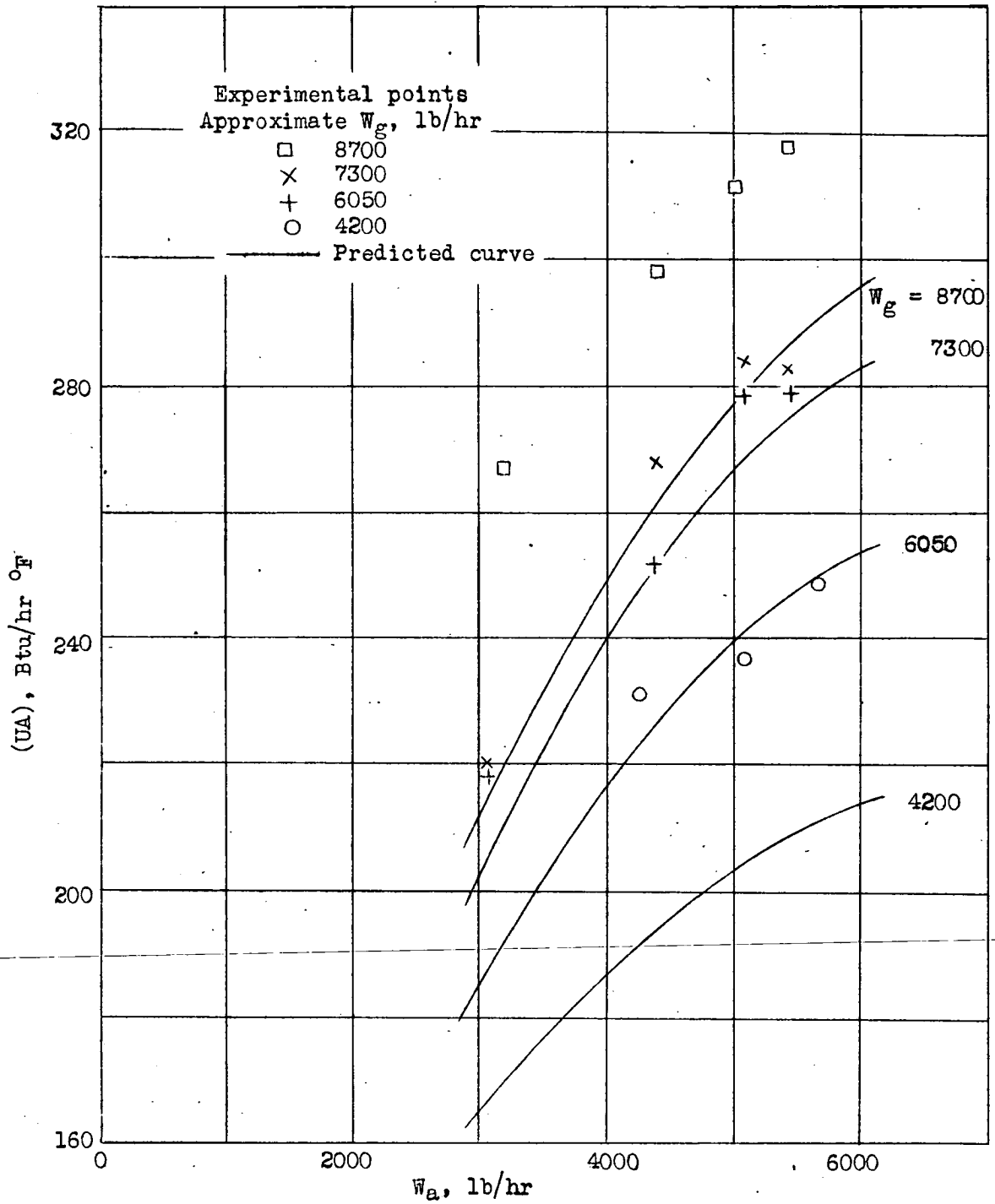


Figure 18.- Overall conductance (UA) of Airesearch fluted type exhaust gas-air heater as a function of ventilating air rate.

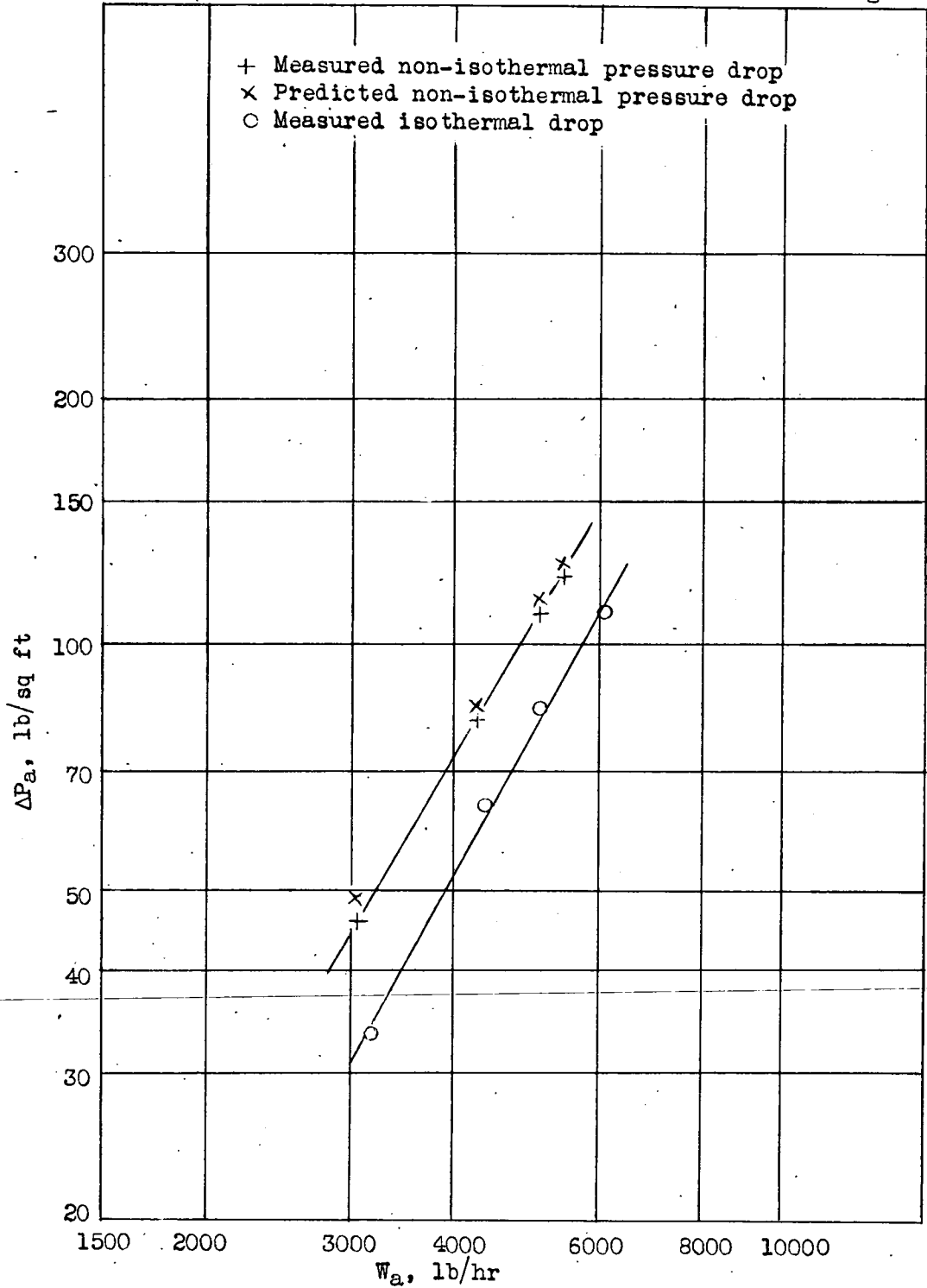


Figure 19.- Pressure drop on air side of Airesearch heater as a function of ventilating air rate.

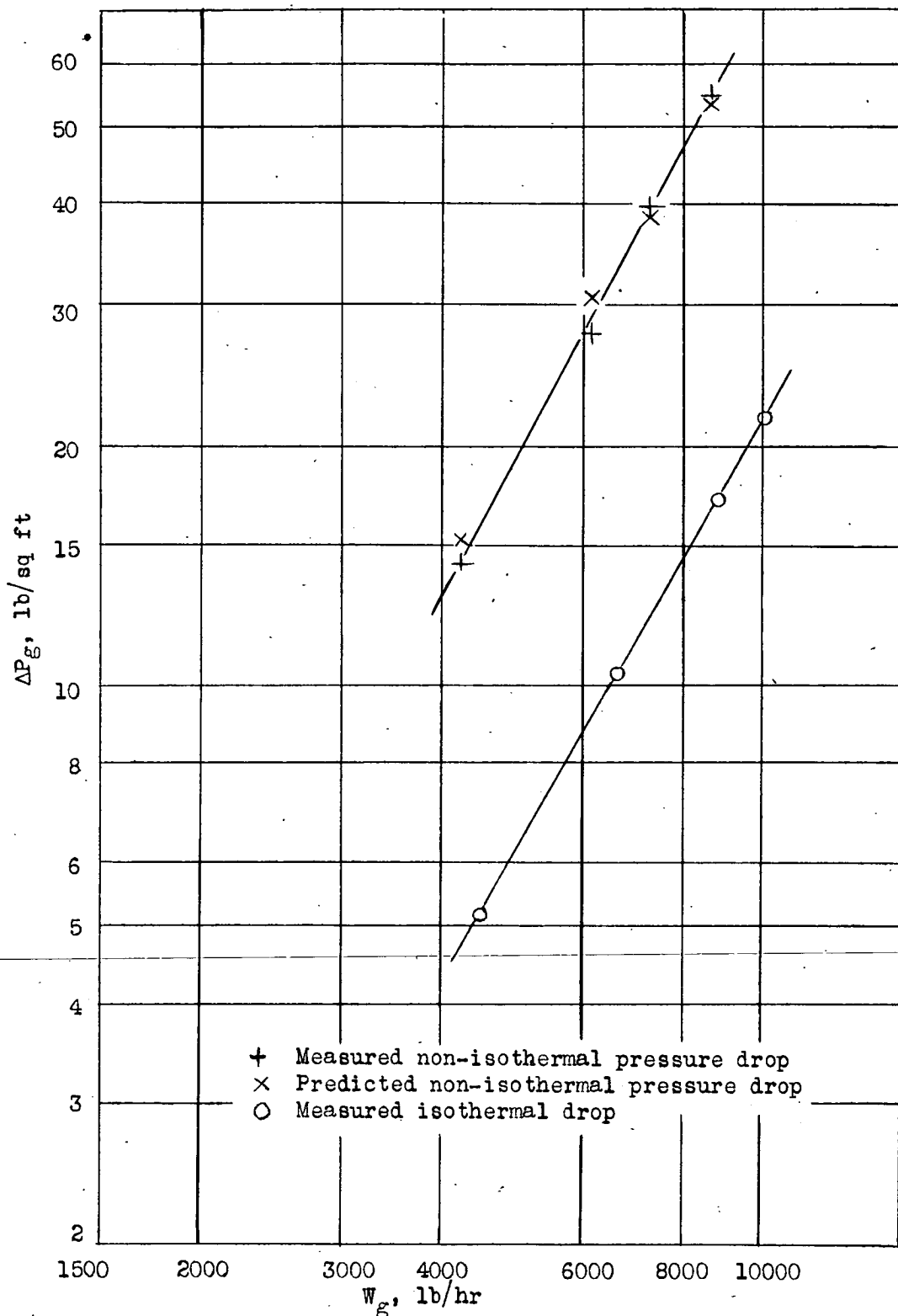


Figure 20.- Pressure on exhaust gas side of Airesearch heater as a function of exhaust gas rate.

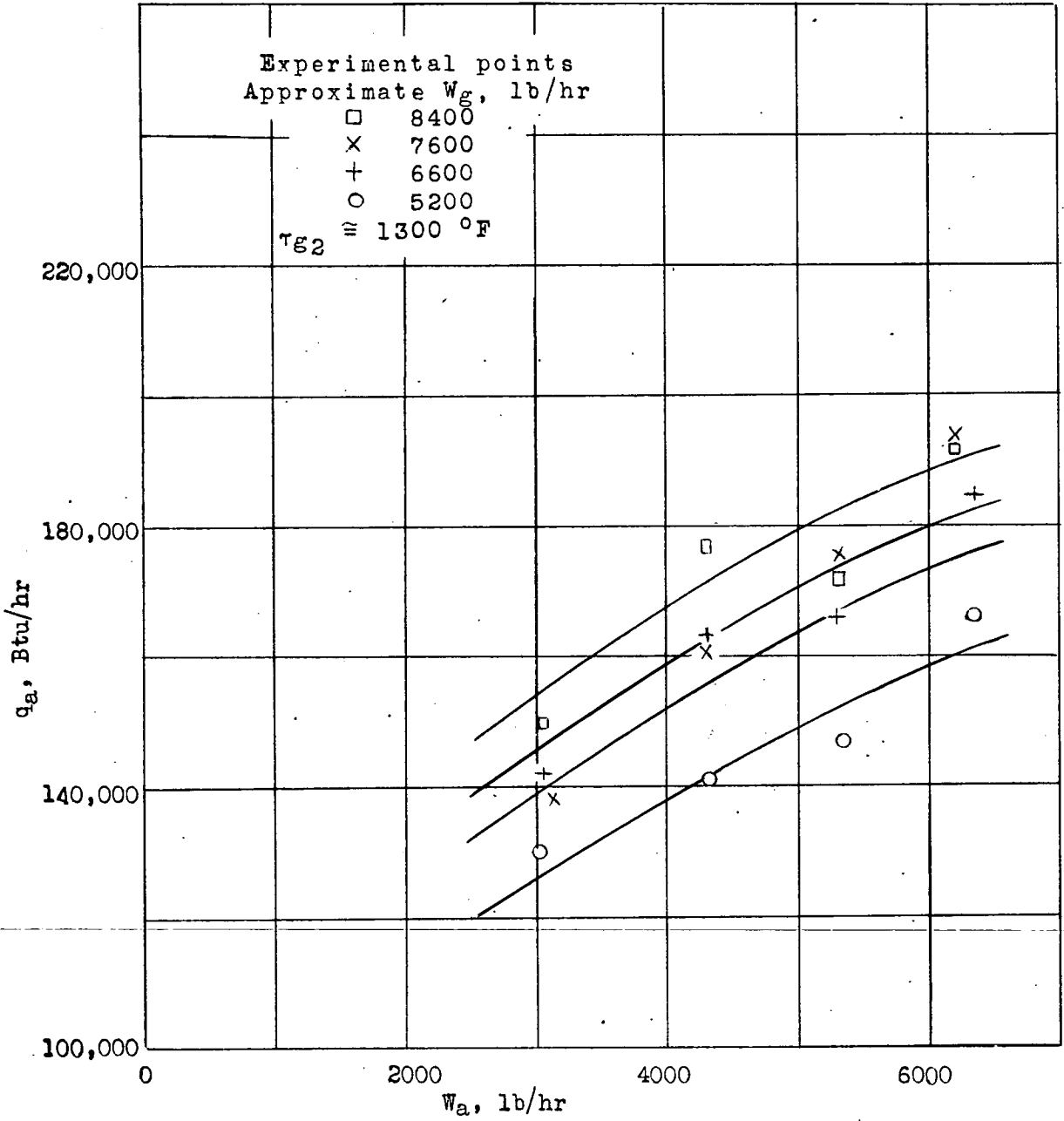


Figure 21 - Thermal output of Solar fluted type exhaust gas-air heater as a function of ventilating air rate.

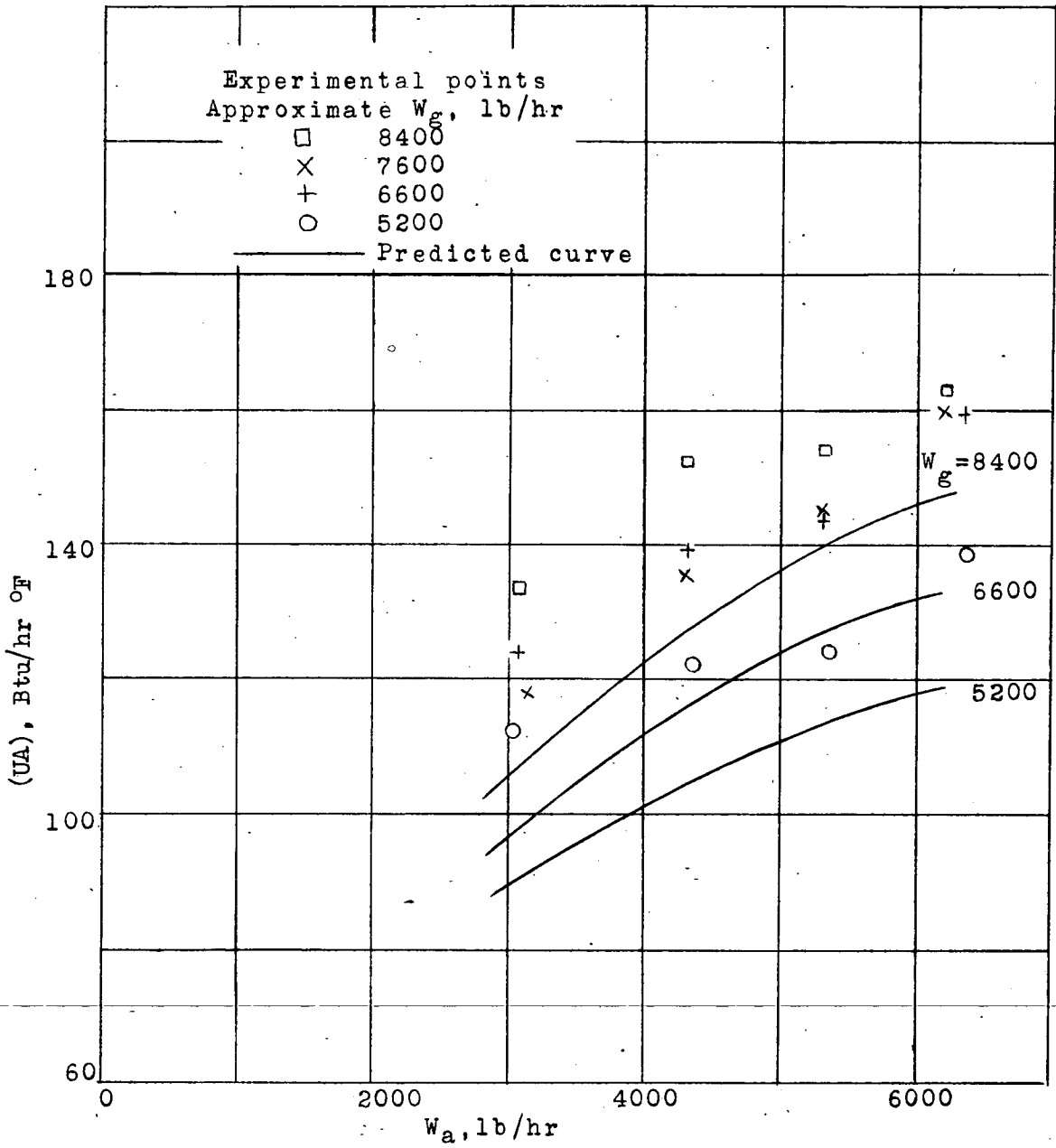


Figure 22.- Overall conductance (UA) of Solar fluted type exhaust gas-air heater as a function of ventilating air rate.

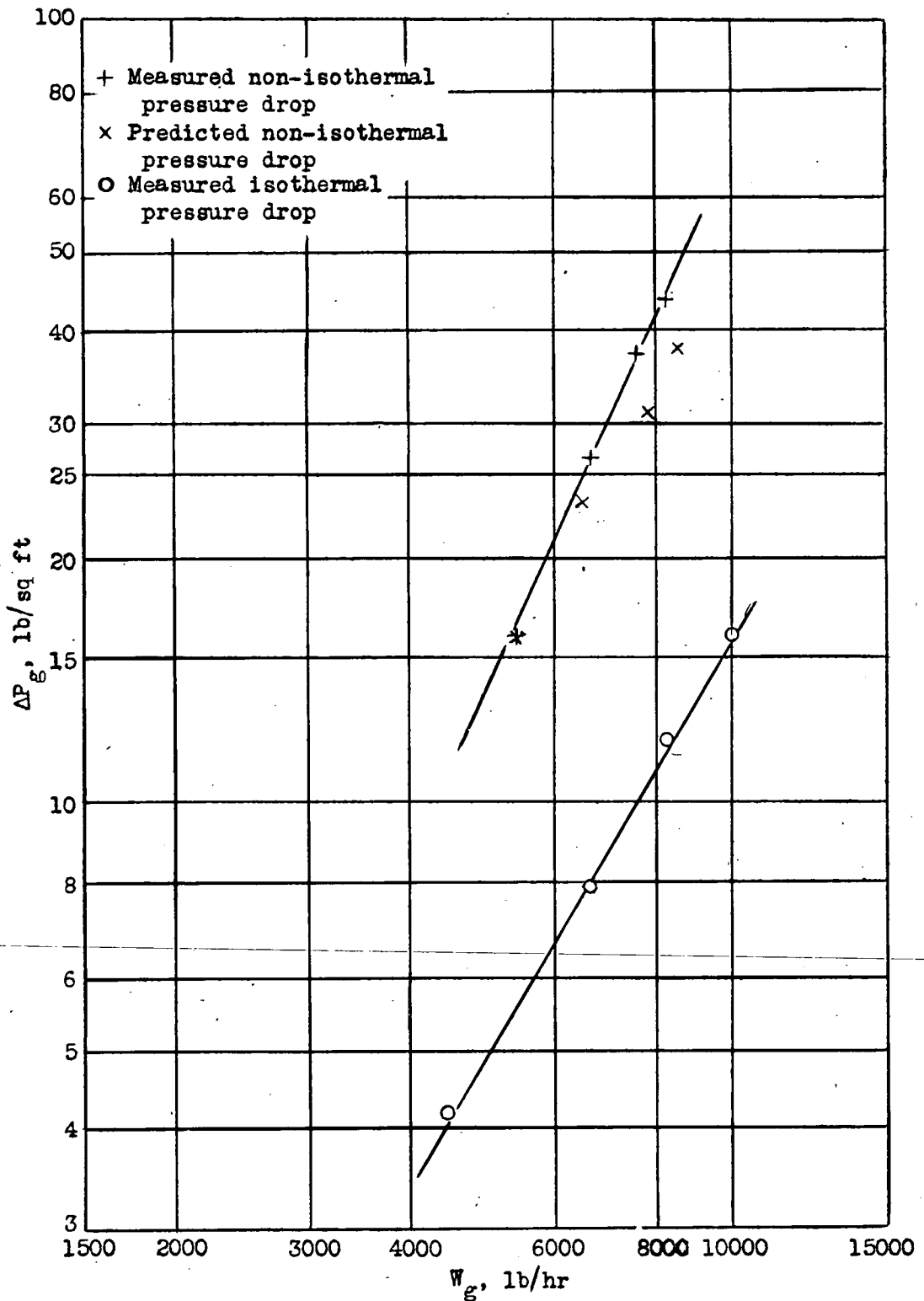


Figure 23.- Pressure drop on exhaust side of Solar heater as a function of exhaust gas rate.

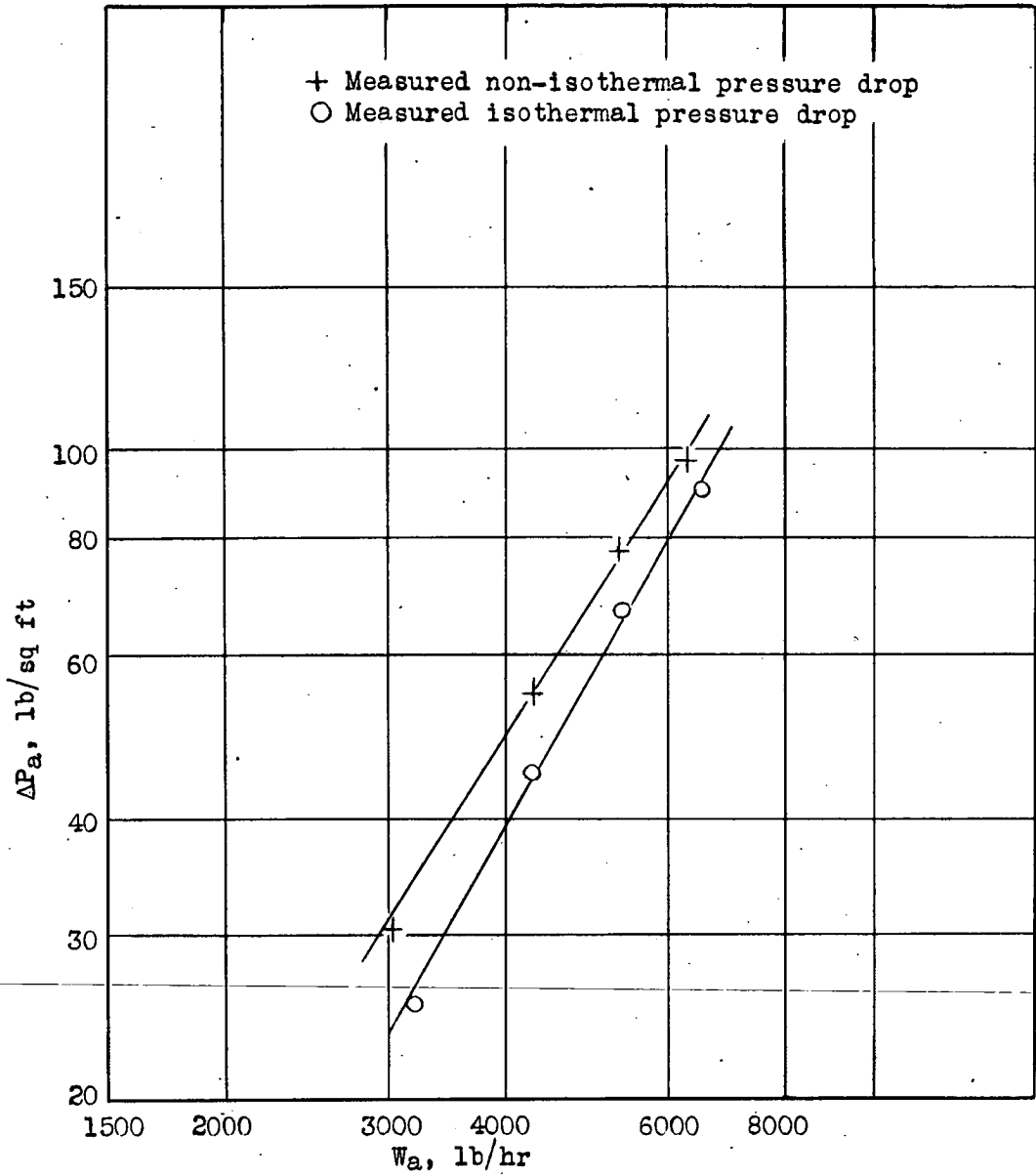


Figure 24.- Pressure drop on the air side of Solar heater as a function of ventilating air rate.